AD-A055 629 PURDUE UNIV LAFAYETTE IND PROJECT SQUID HEADQUARTERS F/G 21/2
EFFECTS OF FINITE REACTION RATE AND MOLECULAR TRANSPORT IN PREM--ETC(U)
MAY 78 P A LIBBY, K N BRAY, J B MOSS N00014-75-C-1143
UNCLASSIFIED SQUIP-UCSD-10-PU NL

| OF |
ADA
055629

END
DATE
FILMED
8-78
DDC

PROJECT SQUID
TECHNICAL REPORT UCSD-10-PU

EFFECTS OF FINITE REACTION RATE AND MOLECULAR TRANSPORT IN PREMIXED TURBULENT COMBUSTION

by

PAUL A. LIBBY
UNIVERSITY OF CALIFORNIA – SAN DIEGO
LA JOLLA, CALIFORNIA
and
K. N. C. BRAY and J. B. MOSS
THE UNIVERSITY OF SOUTHAMPTON
SOUTHAMPTON, ENGLAND

PROJECT SQUID HEADQUARTERS
CHAFFEE HALL
PURDUE UNIVERSITY
WEST LAFAYETTE, INDIANA 47907

MAY 1978

Project SQUID is a cooperative program of basic research relating to Jet Propulsion. It is sponsored by the Office of Naval Research and is administered by Purdue University through Contract N00014-75-C-1143, NR-098-038.

Technical Report UCSD-10-PU

PROJECT SQUID

A COOPERATIVE PROGRAM OF FUNDAMENTAL RESEARCH
AS RELATED TO JET PROPULSION
OFFICE OF NAVAL RESEARCH, DEPARTMENT OF THE NAVY

CONTRACT N00014-75-1143 NR-098-038

EFFECTS OF FINITE REACTION RATE AND MOLECULAR TRANSPORT IN PREMIXED TURBULENT COMBUSTION

BY

Paul A. Libby
University of California-San Diego
La Jolla, California

and

K. N. C. Bray and J. B. Moss
The University of Southampton
Southampton, England

MAY 1978

PROJECT SQUID HEADQUARTERS
CHAFFEE HALL
PURDUE UNIVERSITY
WEST LAFAYETTE, INDIANA 47907

EFFECTS OF FINITE REACTION RATE AND MOLECULAR TRANSPORT IN PREMIXED TURBULENT COMBUSTION

Paul A. Libby
University of California - San Diego, La Jolla, California, U.S.A.

and

K. N. C. Bray and J. B. Moss
The University, Southampton SO9 5NH, England

ABSTRACT

Previous application of the Bray-Moss model for premixed turbulent combustion to planar, oblique and normal flames is extended to include the effect of large but finite values of the two dominant characteristic numbers, a turbulence Reynolds number providing a measure of the intensity of the turbulence and a Damköhler number relating a turbulence time to a chemical time. A classical perturbation analysis involving two small parameters proportional to the inverse of these two numbers is carried out to account separately for the effects of molecular transport and of altered scalar dissipation and for the effects of finite chemical reaction rates. Two limiting cases corresponding to highly oblique confined flames and normal or unconfined oblique flames are treated. Of particular interest in the former case is the effect of the perturbations of the predicted orientation of the

turbulent reaction zone. For the unconfined flames attention focuses on the effect of the perturbations on the turbulent flame speed and on the change in turbulent kinetic energy across the reaction zone. The characteristics of the related laminar flame are introduced so that the theory can conform to the practice of experimentalists in correlating their results for turbulent flame behavior in terms of such laminar flame characteristics. With respect to unconfined flames, for which considerable but often contradictory experimental data are available, the perturbation analysis appears to yield qualitative agreement with a recent correlation of experimental data showing the effect of turbulence Reynolds number. However, a comparison with results of individual experiments is inconclusive.

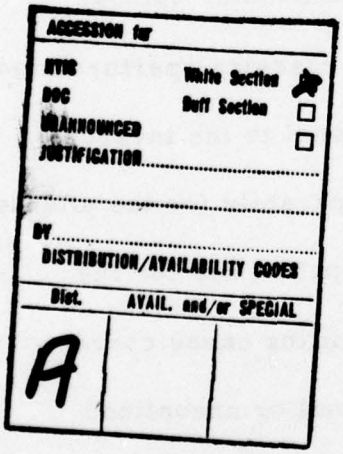

1. INTRODUCTION

Numerous experimental studies of the propagation of turbulent flames into premixed combustible gas mixtures employ the properties of laminar flames to correlate the observed turbulent flame speeds. For example, Abdel-Gayed and Bradley [1] recently presented a correlation of a large amount of experimental data, involving many different combustible mixtures, in which the ratio of turbulent to laminar flame speed is presented as a function of the ratio of laminar flame speed to turbulence intensity and of a turbulence Reynolds number. Other experimental data, for example, that of Wright and Zukoski [2], are insensitive to factors which are known to influence the laminar flame speed. However, it is beyond dispute that a regime exists in which the turbulent flame speed is strongly influenced by the corresponding laminar flame speed.

A successful model of turbulent flames, having any claim to generality, must be able to predict these effects, and must therefore include the relevant fluid mechanical and chemical phenomena. On the other hand, existing models (Borghi and Moreau [3], Pope [4] and Bray and Moss [5, 6]) generally neglect molecular transport and effects of finite rates of combustion reactions, and treat only the limiting case where the time-average rate of heat release is controlled by turbulent mixing. Because the properties of a laminar flame depend

upon a balance between finite rates of molecular transport and chemical reaction, it follows that comparison between predictions from such theories and experiment is at best inadequate and incomplete.

Another problem, of considerable practical importance, is the prediction of the limits of stable combustion. These limits are known to be strongly influenced by chemical kinetic factors, and may also be dependent on Reynolds number, providing a further incentive to improve current combustion models to include these effects.

The objective of the present work is to extend the model of premixed turbulent combustion, developed and exploited by the present authors (Bray and Moss [5, 6], Bray and Libby [7] and Libby and Bray [8]), in order to include effects of a finite reaction rate and of molecular transport, and to compare predicted trends with those observed experimentally. The Bray-Libby and Libby-Bray references will be cited repeatedly and are therefore denoted I and II.

Our presentation is organized as follows: we first review briefly the Bray-Moss model and then discuss the fundamentals required for the inclusion of finite but large values of the two characterizing parameters, a turbulence Reynolds number and a Damköhler number; these are taken to be infinite in previous applications of the model and accordingly lead to a first-order theory. Sections 4 and 5 describe

a perturbation analysis for the two limiting cases of planar flames we consider seminal: highly oblique confined flames and normal or unconfined oblique flames. In the numerical computation of these cases, values for certain parameters are needed. Here we employ the values suggested by a comparison of the predictions of the first order theory with experiment. Section 6 relates the application of the perturbation analysis to current methods of presentation of experimental data and incorporates the relevant laminar flame theory in order to provide estimates for several of the parameters which are thereby encountered. Finally, conclusions are drawn from the analysis.

2. BRIEF DISCUSSION OF THE EXISTING MODEL

For completeness and to provide the requisite background for the developments presented here we discuss the general features of the Bray-Moss model of premixed turbulent reactions and its application to plane flames. Details are in Bray and Moss [5, 6]

and in I. The model utilizes a series of assumptions; some relate to the aerothermochemistry of the flow and are standard in the combustion literature. Of central importance in this regard is the result that the instantaneous thermodynamic state of the reacting mixture depends solely on a reaction progress variable c, in particular

$$T = T(c) = T_o(1 + \tau c) \tag{2.1}$$

$$\rho = \rho(c) = \rho_o(1 + \tau c)^{-1} \tag{2.2}$$

where T is the temperature, ρ is the mixture mass density and the subscript "o" denotes conditions upstream of the reaction zone where $c \equiv 0$. The quantity τ plays an important role in the description of the phenomena; from Eq. (2.1) we note that $\tau = (T_\infty/T_o) - 1$, with T_∞ the temperature downstream of the reaction zone where $c \equiv 1$. Values of τ of practical interest are from 4 to 9. The progress variable c can be considered to be the mass fraction of the product of the one-step reaction normalized by its value when reaction is complete; thus c will usually be loosely termed the product concentration.

A consequence of the dependence of the instantaneous state of the gas mixture on the value of c is that the rate of production of product, i.e., the source term in the conservation equation of product, is also a function of c alone, denoted $w(c)$, with a maximum value w_{max}.

The Bray-Moss model is based on considerations of the probability density function for the concentration c. At a given spatial location within the reaction zone this pdf will involve a partition among unburnt ($c = 0$), burning ($0 < c < 1$), and all burnt ($c = 1$) mixtures. Strengths of α, γ, and β are attributed to each of these respectively. The assumption that the rate of chemical reaction is fast and thus that the rate of heat release is determined by turbulent mixing implies that $\gamma << 1$. Accordingly, the pdf of the concentration c is dominated by delta functions at $c = 0, 1$.

The combination of the dependence of thermochemical quantities on c alone, together with a model for the probability density function for c, permits quantities of fluid mechanical interest to be readily expressed in terms of the mean product concentration, $\tilde{c}$, with corrections of order γ depending on integrals of the pdf denoted $f(c)$ within the interior range $0 < c < 1$. Because it only appears within such integrals, details of $f(c)$ are inessential. Similar considerations apply to the function describing the chemical reaction $w(c)$.

In I and II Favre-averaging is employed (cf. Favre [9]) because of the resulting formal simplification of the describing equations. Thus, for example, we have

$$\overline{\rho c'' c''}/\bar{\rho} = \tilde{c}(1 - \tilde{c}) - \gamma(1 + \tau\tilde{c})M \tag{2.3}$$

$$\bar{w} = w_{max}\gamma I_3 \tag{2.4}$$

$$\overline{c'' w} = \gamma w_{max}(I_4 - \tilde{c} I_3) \tag{2.5}$$

where M and I_k denote integrals of the sort alluded to, namely

$$M = \int_0^1 c(1 - c)(1 + \tau c)^{-1} f(c)\, dc \tag{2.6}$$

$$I_{k+3} = \int_0^1 c^k w(c)\, w_{max}^{-1} f(c)\, dc, \quad k = 0, 1 \tag{2.7}$$

and where $(\tilde{\ })$ and $(\ )''$ denote mass averaged and fluctuating quantities respectively.*

In formalizing the assumption of fast chemistry, it is convenient to introduce a Damköhler number, Da, defined as a ratio of a turbulence time scale to a chemical kinetic time scale, in particular

$$Da = I_3\, w_{max}\, \ell_o / \rho_o \tilde{q}_o^{\frac{1}{2}} \tag{2.8}$$

where ℓ_o is a length scale characterizing the large eddies and $\tilde{q}_o$ is the Favre-averaged turbulent kinetic energy, i.e., $\tilde{q} = \frac{1}{2}\overline{\rho u_\alpha'' u_\alpha''}$. Now for fast chemistry $Da \gg 1$ but $\gamma Da = 0(1)$.

The formulation of the conservation equations based on these assumptions focuses on the equations for turbulent kinetic energy, $\tilde{q}$; the mean product concentration, $\tilde{c}$; and the intensity of the product fluctuations, $\overline{\rho c'' c''}$. A closure problem exists so that some terms must be modelled. At the present time a gradient approximation with an eddy transport coefficient based on the Prandtl-Kolmogoroff model

---

*In the course of the analysis the tilde is also introduced to denote several new variables. No confusion should result.

is employed with a modification to account, at least roughly, for variable density effects. We have (cf. [8])

$$\nu_T = a\tilde{q}^{\frac{1}{2}}\ell_1(\bar{\rho}/\rho_o)^p \tag{2.9}$$

where a is a constant, ℓ_1 is a scale of the large eddies within the reaction zone, and p is an exponent to be assigned. With Eq. (2.9) a typical flux term becomes

$$\overline{\rho u_i'' g''}/\bar{\rho} = -\nu_T(\partial\tilde{g}/\partial x_i) \tag{2.10}$$

In the calculations of I and II molecular transport is neglected, implying consideration of an infinite turbulence Reynolds number,

$$R_T = \tilde{q}_o^{\frac{1}{2}}\ell_o/\nu_o \tag{2.11}$$

where ν is the molecular kinematic viscosity.

There remain to be considered the dissipation of turbulent kinetic energy and of the concentration fluctuations. With respect to the former, denoted $\bar{\varphi}$, the nature of the equations indicates that within the thickness of the reaction zone the dissipation of turbulent kinetic energy must be negligible as is found to be the case when turbulence undergoes rapid distortion (cf., e.g., Batchelor [10]). On the contrary the annihilation of concentration fluctuations by molecular processes is found to be important and is modeled close to the usual fashion, but with variable density effects included, at least roughly; we take

$$\bar{\chi} = C(\bar{\rho}/\rho_o)^k\tilde{q}^{\frac{1}{2}}\overline{\rho c'' c''}/\ell_2 \tag{2.12}$$

where ℓ_2 is another length scale attributed to scalar dissipation and where k is another exponent to be assigned.

The equations which result from these considerations are specialized and subsequently applied to planar turbulent flames. In the case of normal flames and unconfined oblique flames no additional assumptions are required; in the case of confined, oblique flames of specified orientation identified with the angle θ, $\theta = 90^{\circ}$ for normal flames, an additional approximation, namely that the mean streamline is undeflected, results in significant simplification and yet is physically reasonable for confined turbulent flames, e.g., as in Wright and Zukoski [2]. A consequence of this assumption is that there results an explicit expression for the Reynolds stress, i.e., $\overline{\rho u'' v''/\rho}$ in Favre-averaging, in terms of the mean product concentration. An important physical implication which derives from this consideration is that the acceleration through the reaction zone of a confined oblique flame is due to the gradient of Reynolds stress, an implication not based on a gradient assumption but rather on the assumed kinematics of the flow. This contrasts with a normal flame in which the pressure gradient, although thermodynamically negligible, accelerates the gas. The difference in mechanism in the two cases suggests that the appropriate models of the laminar flame within the turbulent reaction zone used to estimate f(c) may likewise be different.

Although for brevity we characterize flames as either oblique or normal, these two cases are considered to correspond respectively to those with constrained and unconstrained mean streamlines, since an

oblique flame involving a constant tangential velocity and thus a curved mean streamline corresponds exactly to a normal flame insofar as our analysis is concerned.

The orientation of the confined flame determines the relative importance of two competing effects related to the interaction of the turbulence and the heat release associated with chemical reaction. If the flame is nearly normal, dilatation dominates and the turbulent kinetic energy downstream of the reaction zone is less than that in the oncoming stream. On the contrary, for oblique flames the generation of turbulent kinetic energy by interaction of the Reynolds stress and the gradient of the mean velocity dominates and the turbulent kinetic downstream exceeds that upstream. This situation leads to an important special case, termed strong interaction, in which the downstream kinetic energy overwhelms that in the oncoming stream.

The resultant mathematical formulation leads to a double eigenvalue problem; the turbulent flame speed in the form $\tilde{u}_o/\tilde{q}_o^{\frac{1}{2}}$ and the ratio of two turbulent kinetic energies, $Q_\infty = \tilde{q}_\infty/\tilde{q}_o$, are predicted for normal flames. In the strong interaction case the ratio of the turbulent flame speed to the turbulent kinetic energy downstream of the flame, $\tilde{u}_o/\tilde{q}_\infty^{\frac{1}{2}}$, and the orientation of the flame θ are given as part of the solution. Thus the mathematical formulation corresponds to a more complex version of that arising in laminar flame theory in which a single eigenvalue, involving chemical kinetic and fluid mechanical quantities, is predicted.

In I and II considerable attention is devoted to comparison between prediction and appropriate experimental results. As indicated earlier this comparison is limited for a variety of reasons including the limitations of the theory. Nevertheless, in II a comparison between the orientation of flames in the strong interaction limit suggests that the two exponents incorporating at least roughly variable density effects in the modelling in the form $(p + k)$ should equal two; the implication from this result is that the usual modelling should be altered when significant density variations occur.

3. INCLUSION OF FINITE DAMKÖHLER AND REYNOLDS NUMBERS

We now consider the extension of the previous application of the Bray-Moss model to planar turbulent flames so as to include finite values for the two characteristic parameters, the Damköhler and Reynolds numbers. The flow we consider is shown schematically in Fig. 1. The Favre-averaged balance equations incorporating the assumptions discussed earlier are as follows:

Continuity:

$$\overline{\rho}\,\tilde{u} = \rho_o \tilde{u}_o \tag{3.1}$$

Species:

$$\overline{\rho}\,\tilde{u}\,\frac{d\tilde{c}}{dx} = \frac{d}{dx}\left(-\overline{\rho c'' u''} + \overline{\rho D \frac{\partial c}{\partial x}}\right) + \overline{w} \tag{3.2}$$

Species fluctuation:

$$\bar{\rho}\,\tilde{u}\,\frac{d}{dx}\left(\frac{\overline{\rho c'' c''}}{\bar{\rho}}\right) - 2\,\overline{\rho c'' u''}\,\frac{d\tilde{c}}{dx} + 2\,\overline{c'' w}$$

$$- \frac{d}{dx}\left(\overline{\rho c'' c'' u''}\right) + 2\,\frac{d}{dx}\left(\overline{\rho D c''\,\frac{\partial c}{\partial x}}\right) - \bar{\chi} \qquad (3.3)$$

Turbulence kinetic energy:

$$\bar{\rho}\,\tilde{u}\,\frac{d\tilde{q}}{dx} = - \overline{\rho u'' u''}\,\frac{d\tilde{u}}{dx} - \overline{\rho u'' v''}\,\frac{d\tilde{v}}{dx}$$

$$- \frac{d}{dx}\left(\tfrac{1}{2}\,\overline{\rho u'' v_\alpha'' v_\alpha''}\right) + \frac{d}{dx}\left(\overline{v_\alpha'' f_{\alpha 1}}\right) - \bar{\varphi} \qquad (3.4)$$

To complete these equations the modelling of the turbulence terms alluded to earlier must be incorporated. In addition, for present considerations the terms associated with the molecular transport coefficient, ρD, and with the viscous stress tensor

$$f_{\alpha\beta} = - \frac{2}{3}\,\mu\,\frac{\partial v_\alpha}{\partial x_\beta}\,\delta_{\alpha\beta} + \mu\left(\frac{\partial v_\alpha}{\partial x_\beta} + \frac{\partial v_\beta}{\partial x_\alpha}\right) \qquad (3.5)$$

and the effect of finite Reynolds numbers on the scalar dissipation must be incorporated. In doing so and in anticipation of a perturbation treatment we introduce a small parameter $\epsilon = (a\,\tilde{q}_o^{\frac{1}{2}}\,\ell_o/\nu_o)^{-1} = (a\,R_T)^{-1}$; a second perturbation parameter will be

$$\delta = (a\,I_3\,w_{max}\,\ell_o/\rho_o\,\tilde{q}_o^{\frac{1}{2}})^{-1} \qquad (3.6)$$

To treat the extra terms we make several additional assumptions:

i) The molecular Schmidt number is taken as unity so that $\rho D = \mu$.

ii) The product $\rho\mu$ is taken as constant so that $\rho\mu = \rho_o\mu_o$, $\nu = \nu_o(1+\tau c)^2$, and $\tilde{\nu} = \nu_o\left((1+\tau\tilde{c})^2 + \tau^2\tilde{c}(1-\tilde{c})\right) + O(\gamma)$.

iii) The scalar dissipation is modified to include a Reynolds number correction so that (cf. Eq. (2.12))

$$\bar{\chi} = C(\bar{\rho}/\rho_o)^k \tilde{q}^{\frac{1}{2}} \overline{\rho c'' c''} \left(1 + (C_1\tilde{\nu}/a\tilde{q}^{\frac{1}{2}}\ell_1)\right)/\ell_2 \tag{3.7}$$

iv) The correlation $\overline{c''(\partial c''/\partial x)}$ is replaced by $\frac{1}{2}\, d/dx\,(\overline{\rho c'' c''}/\bar{\rho})$ with the consequence that

$$\overline{\rho D \frac{\partial c}{\partial x}} \cong \bar{\rho}\tilde{\nu}\frac{d\tilde{c}}{dx} + \frac{d}{dx}\overline{\rho\nu c''} - \tfrac{1}{2}\rho_o\nu_o\tau\frac{d}{dx}\left(\frac{\overline{\rho c'' c''}}{\bar{\rho}}\right)$$

But $\overline{\rho\nu c''} = \rho\nu_o\tilde{c}(1-\tilde{c})\tau(\tau+2) + O(\gamma)$, $\overline{\rho c'' c''}/\bar{\rho} = \tilde{c}(1-\tilde{c}) + O(\gamma)$ so that

$$\overline{\rho D \frac{\partial c}{\partial x}} \cong \bar{\rho}\nu_T \epsilon \left(\frac{\tilde{q}_o^{\frac{1}{2}}\ell_o}{\tilde{q}^{\frac{1}{2}}\ell_1}\right)(1+\tau\tilde{c})^p \left(\frac{\tilde{\nu}}{\nu_o} + \tau\left(\left((1-2\tilde{c}) - \frac{\tilde{c}(1-\tilde{c})\tau}{1+\tau\tilde{c}}\right)(\tau+2) - \tfrac{1}{2}(1-2\tilde{c})(1+\tau\tilde{c})\right)\right)\frac{d\tilde{c}}{dx}$$

$$= \bar{\rho}\nu_T \epsilon R E_1 \frac{d\tilde{c}}{dx} \tag{3.8}$$

where $R = (\tilde{q}_o^{\frac{1}{2}}\ell_o/\tilde{q}^{\frac{1}{2}}\ell_1)$ and where $E_1 = E_1(\tilde{c})$ is implicitly defined. Two contributions to this mean molecular transport term can be identified; the first is associated with the mean

viscosity coefficient, the second with fluctuations in that coefficient. Both can be readily incorporated with the single reasonable assumption cited here.

v) The correlation $\overline{c''c''(\partial c''/\partial x)}$ is replaced with $(1/3)d/dx\,(\overline{\rho c''^3}/\bar{\rho})$ with the consequence that

$$\overline{\rho D c''\frac{\partial c}{\partial x}} = \overline{\rho\nu c''}\,\frac{d\tilde{c}}{dx} + \tfrac{1}{2}\frac{d}{dx}\,\overline{\rho\nu c''^2} - \frac{1}{6}\rho_o\nu_o\tau\,\frac{d}{dx}\left(\frac{\overline{\rho c''^3}}{\bar{\rho}}\right)$$

But $\overline{\rho\nu c''^2} \cong \bar{\rho}\,\nu_o\,\tilde{c}(1-\tilde{c})\left(1+2\tau+\tau^2-\tau(\tau+2)\tilde{c}\right)+O(\gamma)$, $\overline{\rho c''^3}/\bar{\rho} \cong \tilde{c}(1-\tilde{c})(1-2\tilde{c}) + O(\gamma)$ so that

$$\overline{\rho D c''\frac{\partial c}{\partial x}} \cong \bar{\rho}\,\nu_T\,\epsilon R\,(1+\tau\tilde{c})^p\left(\tilde{c}(1-\tilde{c})\tau\left(\tfrac{1}{2}(\tau+2)\right.\right.$$

$$\left. - \tfrac{1}{2}\,\frac{1+2\tau+\tau^2-\tau(\tau+2)\,\tilde{c}}{(1+\tau\tilde{c})} + \frac{1}{3}(1+\tau\tilde{c})\right)\frac{d\tilde{c}}{dx}$$

$$\left. + \tfrac{1}{2}\left(1+2\tau+\tau^2-\tau(\tau+2)\,\tilde{c} - \frac{1}{3}(1+\tau\tilde{c})(1-2\tilde{c})\right)\frac{d}{dx}\left(\frac{\overline{\rho c'' c''}}{\bar{\rho}}\right)\right)$$

$$\cong \bar{\rho}\,\nu_T\,\epsilon R\,E_2\,\frac{d\tilde{c}}{dx} \qquad (3.9)$$

where $E_2(\tilde{c})$ is implicitly defined. Note again that we are able to incorporate without difficulty the molecular transport of fluctuations in concentration due to the mean and fluctuating viscosity coefficient.

vi) The description of the flux of turbulent kinetic energy due to molecular processes as contained in the term $\overline{v_\alpha'' f_{\alpha 1}}$ is more

difficult to rationalize.* However, we incorporate both the effect of fluctuations in the viscosity coefficient and the transport of turbulent kinetic energy by the mean molecular coefficient. Without full justification we take at least provisionally

$$\overline{v_\alpha'' f_{\alpha 1}} = \frac{4}{3}\,\overline{\rho \nu u''}\,\frac{d\tilde{u}}{dx} + \overline{\rho \nu v''}\,\frac{d\tilde{v}}{dx} + \bar{\rho}\,\tilde{\nu}\,\frac{d}{dx}\,\tilde{q} \tag{3.10}$$

The effective transport coefficients $\overline{\rho \nu u''}$ and $\overline{\rho \nu v''}$ can be computed by application of the approach in II involving self-consistent estimates for the velocity components of packets of unburned and fully burned gases within the reaction zone. We find

$$\overline{\rho \nu u''} = -\bar{\rho}\,\nu_T \nu_o \tau(\tau + 2)\,\frac{d\tilde{c}}{dx} + O(\gamma)$$

$$\overline{\rho \nu v''} = -\frac{\bar{\rho}\,\nu_T \nu_o \tau(\tau+2)}{\tan\theta}\,\frac{d\tilde{c}}{dx} + O(\gamma)$$

so that

$$\overline{v_\alpha'' f_{\alpha 1}} = -\bar{\rho}\,\nu_T \epsilon R \left(\left(\frac{4}{3} + \frac{1}{\tan^2\theta} \right) \tilde{u}_o \nu_T \tau^2 (\tau + 2) \left(\frac{d\tilde{c}}{dx} \right)^2 \right.$$

$$\left. - \frac{\bar{\nu}}{\nu_o}\,\frac{d\tilde{q}}{dx} \right) (1 + \tau\tilde{c})^p \tag{3.11}$$

---

*In order to treat the flux of turbulent kinetic energy as thoroughly as that of mean concentration and mean intensity we would need an extension of the Bray-Moss model to a joint velocity-concentration probability density function.

vii) The viscous dissipation $\bar{\varphi}$ is neglected even at finite Reynolds numbers.

With these preliminaries we are prepared to proceed with the treatment of the effects of finite Damköhler and Reynolds numbers.

4. APPLICATION TO THE CASE OF STRONG INTERACTION

We apply the equations which result from imposition of the several considerations discussed earlier to the case of oblique, planar turbulent flames under conditions such that the turbulent kinetic energy generated by shear within the reaction zone overwhelms that in the approaching stream. In this case, which is termed strong interaction, it is convenient to replace $\tilde{q}$ by $\tilde{Q} \equiv (Q - Q_\infty)/(1 - Q_\infty)$, where $Q = \tilde{q}/\tilde{q}_o$. The two eigenvalues which are to be determined as part of the solution and which provide predictions of physical interest are

$$\hat{\beta} = \left(a C \ell_1 / \left((2 c_m - 1) \ell_2 \right) \right) (\tilde{q}_\infty / \tilde{u}_o^2) \tag{4.1}$$

$$\kappa = \tilde{u}_o^2 / \tilde{q}_\infty \tan^2 \theta \tag{4.2}$$

where $c_m \equiv I_4/I_3$. These two eigenvalues determine the turbulent flame speed as a multiple of the turbulent kinetic energy downstream of the flame and the orientation of the flame with respect to the oncoming flow.

For this case Eq. (3.2) becomes

$$\frac{d}{dx} \left(\frac{\bar{\rho} \nu_T}{\rho_o \tilde{u}_o} (1 + \epsilon R E_1) \frac{d\tilde{c}}{dx} \right) = - \frac{\gamma w_{max} I_3}{\rho_o \tilde{u}_o} \tag{4.3}$$

which will prove useful for subsidiary calculations. If Eq. (4.3) is used to eliminate the term involving w_{max} from Eq. (3.3), we have the equation

$$\frac{d}{dx}\left(\frac{\bar{\rho}\nu_T}{\rho_o \tilde{u}_o}\frac{dP}{dx}\right) - \frac{dP}{dx} = (2c_m - 1)\left(\frac{d\tilde{c}}{dx} - \frac{d}{dx}\left(\frac{\bar{\rho}\nu_T}{\rho_o \tilde{u}_o}\frac{d\tilde{c}}{dx}\right)\right.$$

$$\left. - \frac{\hat{\beta}\tilde{u}_o(1-\tilde{Q})\tilde{c}(1-\tilde{c})}{\nu_T(1+\tau\tilde{c})^{1+m}}\left(1 - \frac{P}{\tilde{c}(1-\tilde{c})}\right)\cdot\right.$$

$$\left.\left(1 + \epsilon C_1 R\frac{\tilde{\nu}}{\nu_o}\right)\right) + \epsilon\left(2\frac{d}{dx}\left(\frac{\bar{\rho}\nu_T}{\rho_o \tilde{u}_o} R E_2 \frac{d\tilde{c}}{dx}\right)\right.$$

$$\left. - 2(c_m - \tilde{c})\frac{d}{dx}\left(\frac{\bar{\rho}\nu_T}{\rho_o \tilde{u}_o} R E_1 \frac{d\tilde{c}}{dx}\right)\right) \qquad (4.4)$$

Equation (3.4) becomes

$$\frac{d}{dx}\left(\frac{\bar{\rho}\nu_T}{\rho_o \tilde{u}_o}\frac{d\tilde{Q}}{dx}\right) - \frac{d\tilde{Q}}{dx} = -\left(\frac{\hat{\epsilon}(1-\tilde{Q})\tau}{1+\tau\tilde{c}} - \kappa\tau^2\tilde{c}\right)\frac{d\tilde{c}}{dx}$$

$$- \epsilon\frac{d}{dx}\left(\frac{\bar{\rho}\nu_T}{\rho_o \tilde{u}_o} R\left(\left(\frac{4}{3}\tan^2\theta + 1\right)\frac{\kappa\nu_T\tau^2(\tau+2)}{\tilde{u}_o}\cdot\right.\right.$$

$$\left.\left.\left(\frac{d\tilde{c}}{dx}\right)^2 + \frac{\tilde{\nu}}{\nu_o}\frac{d\tilde{Q}}{dx}\right)(1+\tau\tilde{c})^p\right) \qquad (4.5)$$

where $P = \gamma(1 + \tau\tilde{c})\,M$;

$m = p + k$; and

$\hat{\epsilon} = \frac{1}{2}\overline{\rho u''^2}/\bar{\rho}\tilde{q}$

We now introduce new dependent variables and consider $\tilde{c}$ as the independent variable; let

$$S = (\bar{\rho}\nu_T/\rho_o\tilde{u}_o)(d\tilde{c}/dx)$$

$$G = (\bar{\rho}\nu_T/\rho_o\tilde{u}_o)(d\tilde{Q}/dx) \qquad (4.6)$$

$$D = (\bar{\rho}\nu_T/\rho_o\tilde{u}_o)(dP/dx)$$

The treatment of $\tilde{c}$ as the independent variable implies that the spatial distributions which prevail within the reaction zone may be found a posteriori by quadrature from the first of Eqs. (4.6) to yield $x = x(\tilde{c})$. Equations (4.4) and (4.5) become the following first order equations:

$$\frac{dD}{d\tilde{c}} - \frac{D}{S} = (2c_m - 1)\left(1 - \frac{dS}{d\tilde{c}} - \frac{\hat{\beta}(1-\tilde{Q})\,\tilde{c}(1-\tilde{c})}{S(1+\tau\tilde{c})^{2+m}}\cdot\right.$$

$$\left.\left(1 - \frac{P}{\tilde{c}(1-\tilde{c})}\right)\left(1 + \epsilon C_1 R\,\frac{\tilde{\nu}}{\nu_o}\right)\right)$$

$$+ \epsilon\left(2\frac{d}{d\tilde{c}}(R E_2 S) - 2(c_m - \tilde{c})\frac{d}{d\tilde{c}}(R E_1 S)\right) \qquad (4.7)$$

$$\frac{dP}{d\tilde{c}} = \frac{D}{S} \qquad (4.8)$$

$$\frac{dG}{d\tilde{c}} - \frac{G}{S} = -\left(\frac{\hat{\epsilon}(1-\tilde{Q})\tau}{1+\tau\tilde{c}} - \kappa\tau^2\tilde{c}\right) - \epsilon\frac{d}{d\tilde{c}}\left(R\left(\left(\frac{4}{3}\tan^2\theta+1\right)\kappa \cdot \right.\right.$$

$$\left.\left.\tau^2(\tau+2)(1+\tau\tilde{c})S^2 + \frac{\tilde{\nu}}{\nu_o}G\right)(1+\tau\tilde{c})^P\right) \qquad (4.9)$$

$$\frac{d\tilde{Q}}{d\tilde{c}} = \frac{G}{S} \qquad (4.10)$$

The perturbation equations

Equations (4.7) - (4.10) are in a form suitable for a perturbation analysis. The appropriate expansions are as follows:*

$$\tilde{Q} = \tilde{Q}_o + \epsilon\tilde{Q}_1 + \delta\tilde{Q}_2 + \ldots$$

$$S = S_o + \epsilon S_1 + \delta S_2 + \ldots$$

$$G = G_o + \epsilon G_1 + \delta G_2 + \ldots$$

$$P = \delta(P_o + \ldots)$$

$$D = \delta(D_o + \ldots)$$

$$\hat{\beta} = \hat{\beta}_o + \epsilon\hat{\beta}_1 + \delta\hat{\beta}_2 + \ldots \qquad (4.11)$$

$$\kappa = \kappa_o + \epsilon\kappa_1 + \delta\kappa_2 + \ldots$$

$$\gamma = \delta(\gamma_o + \ldots)$$

$$c_m = c_{mo} + \ldots$$

$$M = M_o + \ldots$$

$$R = R_o + \ldots$$

---

*Although not required at this stage in the analysis, the x-coordinate must also be considered expanded according to $x(\tilde{c}) = x_o(\tilde{c}) + \epsilon x_1(\tilde{c}) + \delta x_2(\tilde{c}) + \ldots$.

Note that not all of these expansions are independent but they are formally consistent as shown.

When Eqs. (4.11) are substituted into Eqs. (4.7)-(4.10), the terms independent of ϵ and δ yield:

$$0 = 1 - \frac{dS_o}{d\tilde{c}} - \frac{\hat{\beta}_o (1 - \tilde{Q}_o)\tilde{c}(1 - \tilde{c})}{S_o (1 + \tau\tilde{c})^{2+m}} \tag{4.12}$$

$$\frac{dG_o}{d\tilde{c}} - \frac{G_o}{S_o} = - \left(\frac{\hat{\epsilon}(1 - \tilde{Q}_o)\tau}{1 + \tau\tilde{c}} - \kappa_o \tau^2 \tilde{c} \right) \tag{4.13}$$

$$\frac{dQ_o}{d\tilde{c}} = \frac{G_o}{S_o} \tag{4.14}$$

which are the equations for the strong interaction case treated in I and II when $\tilde{c}$ is taken as the independent variable. The solutions are subject to boundary conditions which we shall discuss subsequently and yield as eigenvalues $\hat{\beta}_o$ and κ_o.

Collection of the first order terms in ϵ and δ in Eqs. (4.7) - (4.10) yields the following equations, in which for compactness we employ the Kronecker delta δ_{ij}, with $j = 1$ corresponding to the ϵ-perturbation and $j = 2$ to the δ-perturbation:

$$\delta_{i2} \left(\frac{dD_o}{d\tilde{c}} - \frac{D_o}{S_o} \right) = - (2 c_{mo} - 1) \left(\frac{dS_i}{d\tilde{c}} + \left(1 - \frac{dS_o}{d\tilde{c}} \right) \cdot \right.$$

$$\left. \left(\frac{\hat{\beta}_i}{\hat{\beta}_o} - \frac{\tilde{Q}_i}{1 - \tilde{Q}_o} - \frac{S_i}{S_o} - \frac{\delta_{i2} P_o}{\tilde{c}(1 - \tilde{c})} + \delta_{i1} C_1 R_o \frac{\tilde{\nu}}{\nu_o} \right) \right)$$

$$+ \delta_{i1} \left(2 \frac{d}{d\tilde{c}} (R_o E_2 S_o) - 2 (c_{mo} - \tilde{c}) \frac{d}{d\tilde{c}} (R_o E_1 S_o) \right) \tag{4.15}$$

$$\frac{dP_o}{d\tilde{c}} = \frac{D_o}{S_o} \tag{4.16}$$

$$\frac{dG_i}{d\tilde{c}} - \frac{G_o}{S_o}\left(\frac{G_i}{G_o} - \frac{S_i}{S_o}\right) = \left(\frac{\hat{\epsilon}\,\tilde{Q}_i\,\tau}{1+\tau\tilde{c}} + \kappa_o \tau^2 \tilde{c}\left(\frac{\kappa_i}{\kappa_o}\right)\right)$$

$$- \delta_{i1}\frac{d}{d\tilde{c}}\left(R_o\left(\left(\frac{4}{3}\tan^2\theta_o + 1\right)\kappa_o \cdot \right.\right.$$

$$\left.\left.\tau^2(\tau+2)(1+\tau\tilde{c})S_o^2 + \frac{\tilde{\nu}}{\nu_o}G_o\right)(1+\tau\tilde{c})^p\right) \tag{4.17}$$

$$\frac{d\tilde{Q}_i}{d\tilde{c}} = \frac{G_o}{S_o}\left(\frac{G_i}{G_o} - \frac{S_i}{S_o}\right) \tag{4.18}$$

For the perturbation solutions corresponding to finite Reynolds numbers, i.e., to ϵ, $i = 1$, Eqs. (4.15), (4.17), and (4.18) are three equations for S_1, G_1, and $\tilde{Q}_1$. For the perturbation solutions corresponding to finite Damköhler numbers, i.e., to δ, $i = 2$, we must evaluate P_o and D_o. Equation (4.3) and the definition of P lead to

$$P_o = \frac{(1-\tilde{Q}_o)\tilde{c}(1-\tilde{c})}{(1+\tau\tilde{c})^k} R_o\left(\frac{\Phi M_o \tilde{q}_\infty}{\tilde{q}_o}\right) \tag{4.19}$$

where $\Phi = \left(aC\ell_1/(2c_{mo}-1)\ell_2\right)$, taken to be constant. The parameter

Φ appears in I and II and contains several empirical constants evaluated from the phenomenology of turbulence for constant density flows. Equations (4.19) and Eq. (4.16) determine D_o so that the left side of Eq. (4.15) can be expressed in terms of the first order solution. Thus again Eqs. (4.15), (4.17) and (4.18) become three equations, in this case, for S_2, G_2, and $\tilde{Q}_2$.

Note that the last factor in Eq. (4.19) involves explicitly the ratio of the turbulent kinetic energies downstream and upstream of the reaction zone, a ratio large compared to unity in the strong interaction case being considered here. However, we avoid specifying this ratio a priori by introducing a new parameter, $\mathcal{M}_o = (\Phi M_o \tilde{q}_\infty / \tilde{q}_o)$.

The boundary conditions

In terms of the spatial coordinate x, boundary conditions are imposed at $\pm\infty$ which correspond in terms of $\tilde{c}$ to 0, 1. In addition our basic formulation involves the well-known "cold boundary problem" which requires for its resolution specification of a value of $\tilde{c} = \tilde{c}_o$; for $\tilde{c} < \tilde{c}_o$ no chemical reaction occurs.* In the present context this condition corresponds to specification of a mean ignition temperature. In I it is shown that for the highly oblique flames associated with the strong interaction case, the characteristics of the flame are essentially independent of $\tilde{c}_o$, a physically satisfying result.

*This condition implies that at $\tilde{c} = \tilde{c}_o$ the dependent variables are continuous but with "jumps" in their derivatives.

Since the describing equations both for the first order and perturbed solutions can be readily solved for $0 \le \tilde{c} \le \tilde{c}_o \ll 1$, our boundary conditions effectively apply at $\tilde{c}_o$, 1.

Consider the solutions in the range $0 \le \tilde{c} \le \tilde{c}_o \ll 1$; if the right side of Eq. (4.3) is set to zero, we find

$$S_o = \tilde{c} \tag{4.20}$$

and subsequently from Eq. (4.15)

$$S_1 = \left(\frac{2}{3} + 2\tau + \tau^2 - 2c_{mo}\left(1 + \tau\left(\tau + \frac{3}{2}\right)\right)\right) \tilde{c}/(2c_{mo} - 1) \tag{4.21}$$

$$S_2 = 0 \tag{4.22}$$

Furthermore, Eqs. (4.13) and (4.14), simplified as appropriate for $\tilde{c} \sim 0$, $\tilde{Q}_o \sim 1$, yield

$$G_o = -(1 - \tilde{Q}_o) \tag{4.23}$$

Similarly, if Eqs. (4.17) and (4.18) are combined, quadrature leads to the result

$$G_i - \tilde{Q}_i = -G_o, \quad i = 1 \tag{4.24}$$

$$= 0, \quad i = 2 \tag{4.25}$$

provided it is recognized that $R_o \sim 1$.

Equations (4.20) and (4.23), applied at $\tilde{c} = \tilde{c}_o$, provide the boundary conditions for the first order solutions already presented in I and II and

determine the eigenvalues $\hat{\beta}_o$ and κ_o. Likewise, as we shall see, the pairs of equations, Eqs. (4.21) and (4.24) and (4.22) and (4.25), determine the perturbation eigenvalues.

The boundary conditions to be imposed at the other end of the range of $\tilde{c}$, i.e., in the neighborhood of $\tilde{c} = 1$, are more complex; their detailed consideration is discussed in Appendix 1. For present purposes it is sufficient to note that the asymptotic behavior of the first order and perturbation solutions as $\tilde{c} \sim 1$ is such that no arbitrariness is involved. Accordingly, a numerical integration initiated in the neighborhood of $\tilde{c} = 1$ can be carried out for decreasing $\tilde{c}$ with the boundary conditions at $\tilde{c} = \tilde{c}_o$ satisfied by appropriate selection of the eigenvalues. The numerical analysis of the first order solutions requires iteration since the asymptotic solutions as $\tilde{c} \sim 1$ involve the eigenvalues. However, the perturbation solutions can be generated in a form such that only a single integration from the neighborhood of $\tilde{c} \sim 1$ to $\tilde{c} \sim \tilde{c}_o$ is required.

Treatment of the perturbation equations involves specification of a form for the quantity R_o which is the ratio of products of a length scale and the square root of the turbulent kinetic energy. This situation is in contrast to that prevailing for the first order solutions; in terms of the mean product concentration these can be determined without specification of a length scale model. Here for simplicity and with the expectation that our conclusions will not be affected by more complex models, we take $R_o \equiv 1$ which implies that the length

scale is inversely proportional to the square root of the turbulent kinetic energy.

The form of the perturbation solutions

In addition to the parameters which determine the first order solutions, namely τ, $\hat{\epsilon}$, m, and $\tilde{c}_o$, we must specify for the perturbation solutions the individual contributions to m, i.e., p and k, the parameters Φ and c_{mo}, and the coefficients C_1 and $\mathcal{M}_o$. However, it is possible to carry out the numerical analysis of the perturbation solutions so that for given first order solutions only one integration is required without a priori specification of C_1 and $\mathcal{M}_o$. To illustrate consider the solutions for $\tilde{Q}_i$ in the form

$$\tilde{Q}_i = \delta_{i1}\tilde{Q}_{ip} + \left(\frac{\hat{\beta}_i}{\hat{\beta}_o}\right)\tilde{Q}_{i1} + \left(\frac{\kappa_i}{\kappa_o}\right)\tilde{Q}_{i2} + \delta_{i1}C_1\tilde{Q}_{i3} + \delta_{i2}\mathcal{M}_o\tilde{Q}_{i3}, \quad i = 1, 2 \tag{4.26}$$

where $\tilde{Q}_{in} = \tilde{Q}_{in}(\tilde{c})$, n = p, 1, 2, 3 provide the constituent parts of the perturbation solution $\tilde{Q}_i(\tilde{c})$. Similar expressions prevail for S_i and G_i. When these forms are substituted into Eqs. (4.21) and (4.24) for i = 1 and into Eqs. (4.22) and (4.25) for i = 2 with $\tilde{c} = \tilde{c}_o$, we obtain for each perturbation two algebraic equations for the two pairs of eigenvalues in the form $(\hat{\beta}_i/\hat{\beta}_o)$, (κ_i/κ_o). Values for C_1 and $\mathcal{M}_o$ are required if specific values for the perturbation eigenvalues are desired. However, the solutions to the algebraic equations can be arranged to yield

$$\hat{\beta}_1/\hat{\beta}_o = a_{11} + C_1 b_{11} \tag{4.27}$$

$$\kappa_1/\kappa_o = a_{12} + C_1 b_{12} \tag{4.28}$$

$$\hat{\beta}_2/\hat{\beta}_o = \mathcal{M}_o b_{21} \tag{4.29}$$

$$\kappa_2/\kappa_o = \mathcal{M}_o b_{22} \tag{4.30}$$

where the a_{ij} and b_{ij} coefficients are known and depend only on the first order solution, on the parameters p and k, and on Φ and c_{mo}. It is thus possible to assess readily the sensitivity of the perturbation eigenvalues to the extra parameters C_1 and $\mathcal{M}_o$.

The form of Eqs. (4.27) - (4.30) warrants comment. The perturbation eigenvalues corresponding to large but finite values of the Reynolds number are due to two separate effects; the a_{11} and a_{12} coefficients arise from the molecular transport terms in the conservation equations. A second effect is contained in the b_{11} and b_{12} coefficients and is associated with the parameter C_1 and thus with the influence of Reynolds numbers on the scalar dissipation.

The situation regarding the influence of finite but large Damköhler numbers is different and is seen to be associated with the parameter $\mathcal{M}_o$ alone. According to the present analysis $\mathcal{M}_o$ is proportional to the ratio of turbulent kinetic energies, $(\tilde{q}_\infty/\tilde{q}_o)$ with the proportionality factor depending on M_o, i.e., on an integral of the distribution of product through the reacting surfaces in the form $f(c)$.

The physical significance of the perturbation eigenvalues

Of primary interest from the numerical results is the effect of large but finite values of the Reynolds and Damkohler numbers, on the turbulent flame speed in the form $(\tilde{u}_o/\tilde{q}_\infty^{\frac{1}{2}})$ and on the orientation of the flame, i.e., on θ. The definitions of $\hat{\beta}$ and κ (cf. Eqs. (4.1) and (4.2)) yield*

$$(\tilde{u}_o/\tilde{q}_\infty^{\frac{1}{2}})_i = -\tfrac{1}{2}\,(\tilde{u}_o/\tilde{q}_\infty^{\frac{1}{2}})_o\,(\hat{\beta}_i/\hat{\beta}_o) \tag{4.31}$$

$$\theta_i = -\tfrac{1}{2}\left(\frac{\tan\theta_o}{1+\tan^2\theta_o}\right)\left(\frac{\hat{\beta}_i}{\hat{\beta}_o}+\frac{\kappa_i}{\kappa_o}\right) \simeq -\tfrac{1}{2}\,\theta_o\left(\frac{\hat{\beta}_i}{\hat{\beta}_o}+\frac{\kappa_i}{\kappa_o}\right) \tag{4.32}$$

for $i = 1, 2$.

Numerical Results

The first-order solutions require only values of the heat release parameter τ and of $\tilde{c}_o$, and m; we have assumed a range of values for τ but taken $\hat{\epsilon} = 0.3$ and $m = 2$ as in I and II. For one case several values for $\tilde{c}_o$ are assumed to demonstrate the relative insensitivity of our results to the "cold boundary" condition. The perturbation solutions on the other hand require specification of other parameters; in addition to the eigenvalues $\hat{\beta}_o$ and κ_o the angle θ_o appears and therefore a value for Φ is required. Also required are values for c_{mo} and for the individual components of m, i.e., for p

---

*Equation (4.31) is based on the assumption that the factor multiplying $(\tilde{q}_\infty/\tilde{u}_o^2)$ in Eq. (4.1) is invariant with respect to the perturbation parameters and therefore equal to Φ.

and k. Subsequent applications of the perturbation solutions with these quantities specified require values for C_1 and $\mathcal{M}_o$. Without complete rationalization we take $p = k = 1$ while for Φ we take the strong interaction value given in Appendix 3: $\Phi = 0.1$. Generally we assume c_{mo} to be 0.833 but show with one calculation the effect associated with $c_{mo} = 0.75$. Note that in Appendix 2 we discuss the elements of laminar flame theory used to establish these values which are close to the value of $c_{mo} = 0.7$ used in I and II.

The asymptotic approximations to the first order solutions in the neighborhood of $\tilde{c} = 1$ are applied at $\tilde{c} = 0.95$. It is found necessary to initiate the integration of the perturbation solutions closer to $\tilde{c} \sim 1$ in order to achieve satisfactory accuracy; accordingly, we take $\tilde{c} = 0.98$ as the starting point for the perturbation solutions.

For purposes of exposition we consider the case $\tau = 5$, $\tilde{c}_o = 0.02$, $c_{mo} = 0.833$ to be prototypical and display the results therefor. In Fig. 2 we show the first order solutions. For this case $\hat{\beta}_o = 87.2$, $\kappa_o = 0.0897$ and the angle θ_o is found to be 6.45^o. In Figs. 3 and 4 we show the perturbation solutions for Reynolds and Damköhler numbers respectively. For the former we take $C_1 = 1$, an indicative value.

The perturbation eigenvalues provide the results of greatest physical significance from this analysis. In Table 1 we show results for several cases, i.e., for several values of τ and $\tilde{c}_o$ and c_{mo}. Presented are the coefficients a_{ij}, b_{ij} (cf. Eqs. (4.27)-(4.30)) from which the ratios $(\hat{\beta}_i/\hat{\beta}_o)$ and (κ_i/κ_o) may be computed. Also shown

are the ratios of the physically significant quantities $(\tilde{u}_o/\tilde{q}_\infty^{\frac{1}{2}})_i/(\tilde{u}_o/\tilde{q}_\infty^{\frac{1}{2}})_o$ and θ_i (cf. Eqs. (4.31) and (4.32)). For the ϵ-perturbations we have again taken $C_1 = 1$.

Although we shall discuss the implications from these results in detail in Section 6, it is perhaps appropriate to make several remarks. Note that apparently the greatest sensitivity of the turbulent flame speed and of the orientation of the flame is associated with the influence of molecular transport, i.e., with the ϵ-perturbations. The extent of this influence depends on the heat release, decreasing as τ decreases. In fact for $\tau = 5$ it appears that the first term in the series in ϵ cannot be continued beyond $\epsilon = 10^{-2}$ without raising doubt as to the validity of the perturbation analysis. A value of $\epsilon = 10^{-2}$ corresponds to $R_T \simeq 10^3$ if our standard value of a, namely 0.09, is assumed. Note that the effect of finite Damköhler numbers increases as τ decreases and that the perturbation results are relatively insensitive to the value of c_{mo}.

The influence of finite Damköhler numbers on flame properties depends directly on the magnitude of the parameter $\mathcal{M}_o$. However, values thereof on the order of 10^4 appear to be required in order for the influence of finite reaction rate to be comparable to that of finite Reynolds numbers. In addition the κ_2-eigenvalues are exceedingly small. Thus the changes in the orientation of the flame due to finite Damköhler effects are due essentially to the $\hat{\beta}_2$-eigenvalues.

5. APPLICATION TO NORMAL FLAMES

We now apply the same techniques used for flames undergoing strong interaction to flames involving only dilatation due to heat release, i.e., either to normal flames, or to unconfined, oblique flames. Because the treatment closely follows that in the previous section, we need only outline the steps in the analysis. In this case the turbulent kinetic energy is conveniently replaced by $\tilde{Q}$ where $\tilde{q} = \tilde{q}_o \left((1 - Q_\infty) \tilde{Q} + \tilde{Q}_\infty \right)$ while the two eigenvalues to be determined as part of the solution are conveniently taken to be

$$\tilde{\beta} = \left(a C \ell_1 / (2c_m - 1) \ell_2 \right) (\tilde{q}_o / \tilde{u}_o^2) (1 - Q_\infty) \tag{5.1}$$

$$\hat{Q} = Q_\infty / (1 - Q_\infty) \tag{5.2}$$

The quantities $\tilde{\beta}$ and $\hat{Q}$ determine the turbulent flame speed in the form $(\tilde{u}_o / \tilde{q}_o^{\frac{1}{2}})$ and the ratio of the turbulent kinetic energies downstream and upstream of the flame, i.e., Q_∞.

Equations (3.1) - (3.4) with the modelling and representation of the molecular transport terms associated with Eqs. (3.6) - (3.8) provide the starting point for the analysis. With $\theta = 90^o$ and with the alterations of the equations as a result of the different eigenvalues, Eqs. (4.3) - (4.5) are changed in obvious ways. Finally, if the new dependent variables given by Eqs. (4.6) are introduced and again $\tilde{c}$ is treated as the independent variable, we find the following first order equations:

$$\frac{dD}{d\tilde{c}} - \frac{D}{S} = (2c_m - 1)\left(1 - \frac{dS}{d\tilde{c}} - \frac{\tilde{\beta}(\tilde{Q} + \hat{Q})\tilde{c}(1-\tilde{c})}{S(1+\tau\tilde{c})^{2+m}} \cdot \right.$$

$$\left. \left(1 - \frac{P}{\tilde{c}(1-\tilde{c})}\right)\left(1 + \epsilon C_1 R \frac{\tilde{\nu}}{\nu_o}\right)\right) + \epsilon\left(2\frac{d}{d\tilde{c}}(R E_2 S)\right.$$

$$\left. - 2(c_m - \tilde{c})\frac{d}{d\tilde{c}}(R E_1 S)\right) \tag{5.3}$$

$$\frac{dP}{d\tilde{c}} = \frac{D}{S} \tag{5.4}$$

$$\frac{dG}{d\tilde{c}} - \frac{G}{S} = \frac{\hat{\epsilon}\tau}{1+\tau\tilde{c}}(\tilde{Q} + \dot{Q}) + \epsilon\frac{d}{d\tilde{c}}\left(R\left(\frac{4}{3}\frac{\Phi(1+\tau\tilde{c})}{\tilde{\beta}}\right.\right.$$

$$\left.\left. \tau^2(\tau+2)S^2 - \frac{\tilde{\nu}}{\nu_o} G\right)(1+\tau\tilde{c})^P\right) \tag{5.5}$$

$$\frac{d\tilde{Q}}{d\tilde{c}} = \frac{G}{S} \tag{5.6}$$

The same perturbation parameters ϵ and δ are retained. These equations are consistent with Eqs. (4.7) - (4.10) if $\kappa = 0$ and if Q_∞ becomes indefinitely large; note that $\hat{Q} \sim -1$ and $\tilde{\beta}\hat{Q} \sim \hat{\beta}$ if $Q_\infty \sim \infty$.

The perturbation equations

The expansions given by Eqs. (4.11) are again employed with those for $\hat{\beta}$ and κ replaced by

$$\tilde{\beta} = \tilde{\beta}_o + \epsilon\tilde{\beta}_1 + \delta\tilde{\beta}_2 + \ldots$$

$$\hat{Q} = \hat{Q}_o + \epsilon\hat{Q}_1 + \delta\hat{Q}_2 + \ldots \tag{5.7}$$

When all of the expansions are substituted into Eqs. (5.3) - (5.6), the terms independent of ϵ and δ yield

$$0 = 1 - \frac{dS_o}{d\tilde{c}} + \frac{\tilde{\beta}_o(\tilde{Q}_o + \hat{Q}_o)\tilde{c}(1 - \tilde{c})}{S_o(1 + \tau\tilde{c})^{2+m}} \tag{5.8}$$

$$\frac{dG_o}{d\tilde{c}} - \frac{G_o}{S_o} = \hat{\epsilon}(\tilde{Q}_o + \hat{Q}_o)\ \frac{\tau}{1 + \tau\tilde{c}} \tag{5.9}$$

$$\frac{d\tilde{Q}_o}{d\tilde{c}} = \frac{G_o}{S_o} \tag{5.10}$$

Equations (5.8) - (5.10) are essentially those treated in I with the changes due to redefined eigenvalues and to the introduction of variable density effects via the exponent m.

Collection of the first order terms in ϵ and δ from Eqs. (5.3) - (5.6) yield the equations for the perturbation solutions, namely

$$\delta_{i2}\left(\frac{dD_o}{d\tilde{c}} - \frac{D_o}{S_o}\right) = -(2c_{mo} - 1)\left(\frac{dS_i}{d\tilde{c}} + \left(1 - \frac{dS_o}{d\tilde{c}}\right)\cdot\right.$$

$$\left(\frac{\tilde{\beta}_i}{\tilde{\beta}_o} + \frac{\tilde{Q}_i + \hat{Q}_i}{\tilde{Q}_o + \hat{Q}_o} - \frac{S_i}{S_o} - \delta_{i2}\ \frac{P_o}{\tilde{c}(1 - \tilde{c})}\right.$$

$$\left.\left. + \delta_{i1} C_1 R_o \frac{\tilde{\nu}}{\nu_o}\right)\right) + \delta_{i1}\left(2\frac{d}{d\tilde{c}}(R_o E_2 S_o)\right.$$

$$\left. - 2(c_{mo} - \tilde{c})\ \frac{d}{d\tilde{c}}(R_o E_1 S_o)\right) \tag{5.11}$$

$$\frac{dP_o}{d\tilde{c}} = \frac{D_o}{S_o} \tag{5.12}$$

$$\frac{dG_i}{d\tilde{c}} - \frac{G_o}{S_o}\left(\frac{G_i}{G_o} - \frac{S_i}{S_o}\right) = \frac{\hat{\epsilon}\tau}{1+\tau\tilde{c}}\,(\tilde{Q}_i + \hat{Q}_i)$$

$$+ \delta_{i1}\frac{d}{d\tilde{c}}\left(R_o\left(\frac{4}{3}\,\frac{\Phi(1+\tau\tilde{c})\tau^2(\tau+2)S_o^2}{\tilde{\beta}_o} - \frac{\tilde{\nu}}{\nu_o}G_o\right)(1+\tau\tilde{c})^P\right) \tag{5.13}$$

$$\frac{dQ_i}{d\tilde{c}} = \frac{G_o}{S_o}\left(\frac{G_i}{G_o} - \frac{S_i}{S_o}\right) \tag{5.14}$$

where again we use the Kronecker delta for compactness: $i = 1$ for the ϵ-perturbations, $i = 2$ for the δ-perturbations.

The considerations made previously regarding the determination of the two sets of perturbation solutions by these equations apply in this case. However, in place of Eq. (4.19) we find for the function P_o

$$P_o = \frac{R_o(\tilde{Q}_o + \hat{Q}_o)\tilde{c}(1-\tilde{c})}{(1+\tau\tilde{c})^k}\left(\Phi M_o(1 - Q_{\infty o})\right) \tag{5.15}$$

For convenience we introduce $\hat{M} = \Phi M_o(1 - Q_{\infty o})$ and consider it to be a parameter in the perturbation solutions.

The boundary conditions

The previous comments concerning specification of boundary conditions at $\tilde{c} = \tilde{c}_o$ and in the neighborhood of $\tilde{c} \sim 1$ apply here as well. We should note, however, that as shown in I the results for first

order solutions for normal flames depend somewhat on the value of $\tilde{c}_o$; this is interpreted as indicating the dependence of turbulent flame speed for normal flames on the method of flame stabilization. Accordingly, we expect the perturbation eigenvalues to be somewhat dependent on $\tilde{c}_o$.

The solutions for the range $0 \leq \tilde{c} \leq \tilde{c}_o \ll 1$ are given by Eqs. (4.20) - (4.22) but Eqs. (4.23) - (4.25) are replaced by

$$G_o = -(1 - \tilde{Q}_o) + \hat{\epsilon}\tau(1 + \hat{Q}_o)\tilde{c} \tag{5.16}$$

$$G_i - \tilde{Q}_i = -G_o + \hat{\epsilon}\tau\,\hat{Q}_i\,\tilde{c}, \qquad i = 1 \tag{5.17}$$

$$= \hat{\epsilon}\tau\,\hat{Q}_i\tilde{c}, \qquad i = 2 \tag{5.18}$$

These solutions for the first order equations applied at $\tilde{c} = \tilde{c}_o$ provide the boundary conditions which determine the first order eigenvalues, $\tilde{\beta}_o$ and $\hat{Q}_o$. Similarly, those applicable to the perturbation equations determine the perturbation eigenvalues $\tilde{\beta}_i$ and $\hat{Q}_i$, $i = 1, 2$.

The boundary conditions for the solutions in the neighborhood of $\tilde{c} = 1$ are developed in detail in Appendix 1 and involve no arbitrariness if the solutions are to have acceptable behavior near $\tilde{c} = 1$. Thus integration of both the first order and perturbation solutions is initiated at a value of $\tilde{c}$ suitably close to $\tilde{c} = 1$. For simplicity we repeat our earlier assumption and take the quantity R_o to be unity.

The form of the perturbation solutions and related matters

For normal flames the first order solutions require specification of the parameters τ, $\hat{\epsilon}$, m and $\tilde{c}_o$. Again in this case we seek the

perturbation solutions in a form requiring specification of a minimum number of additional parameters until specific values for the perturbation eigenvalues and until reconstituted perturbation solutions are desired. Thus, for example, we determine the $\tilde{Q}_i$ solutions in the form

$$\tilde{Q}_i = \delta_{i1}\tilde{Q}_{ip} + \left(\frac{\tilde{\beta}_i}{\tilde{\beta}_o}\right)\tilde{Q}_{i1} + \frac{\hat{Q}_i}{\hat{Q}_o}\tilde{Q}_{i2} + \delta_{i1}C_1\tilde{Q}_{i3} + \delta_{i2}\hat{M}\tilde{Q}_{i3} \qquad (5.19)$$

with similar forms for S_i and G_i (cf. Eq. (4.26) and comments applying thereto). When these forms are substituted into Eqs. (4.21) and (5.17) for $i = 1$ and into Eqs. (4.22) and (5.18) for $i = 2$ with $\tilde{c} = \tilde{c}_o$, we obtain two pairs of algebraic equations for the pairs of eigenvalues in the form $(\tilde{\beta}_i/\tilde{\beta}_o)$ and $(\hat{Q}_i/\hat{Q}_o)$. The results are conveniently arranged as in Eqs. (4.27) - (4.30), namely as

$$\tilde{\beta}_1/\tilde{\beta}_o = a_{11} + C_1 b_{11} \qquad (5.20)$$

$$\hat{Q}_1/\hat{Q}_o = a_{12} + C_1 b_{12} \qquad (5.21)$$

$$\tilde{\beta}_2/\tilde{\beta}_o = \hat{M} b_{21} \qquad (5.22)$$

$$\hat{Q}_2/\hat{Q}_o = \hat{M} b_{22} \qquad (5.23)$$

where the a_{ij} and b_{ij} coefficients depend only on the parameters determining the first order solutions and indicate the sensitivity of the perturbation eigenvalues to molecular transport and to the parameters C_1 and $\hat{M}$.

The physically interesting results from this analysis pertain to the perturbed values for the turbulent flame speed and for the ratio of turbulent kinetic energy downstream and upstream of the flame. These are found

from Eqs. (5.1), (5.2) and (5.7) with Φ taken as a constant to be expressible in terms of the perturbation eigenvalues as

$$\left(\frac{\tilde{u}_o}{\tilde{q}_o^{\frac{1}{2}}}\right)_i = -\tfrac{1}{2}\left(\frac{\tilde{u}_o}{\tilde{q}_o^{\frac{1}{2}}}\right)_o \left(Q_{\infty o}\frac{\hat{Q}_i}{\hat{Q}_o} + \frac{\tilde{\beta}_i}{\tilde{\beta}_o}\right) \tag{5.24}$$

$$Q_{\infty i} = Q_{\infty o}(1 - Q_{\infty o})\left(\frac{\hat{Q}_i}{\hat{Q}_o}\right) \tag{5.25}$$

Numerical Results

We have obtained numerical solutions for normal flames based on our standard values of $\hat{\epsilon} = 0.3$, $m = 2$ for a range of values of the heat release parameter τ. Generally, we take $\tilde{c}_o = 0.02$ but for one case we show the influence of different values thereof. As in the strong interaction case the perturbation solutions require specification of additional parameters; generally, we assume $c_{mo} = 0.833$ but again for one case we show the effect of $c_{mo} = 0.75$. The value of Φ is assumed to be 1.4 (cf. Appendix 3). Finally, we again take $p = k = 1$.

The numerical solution of the equations for normal flames is found to be increasingly difficult as τ increases. With the standard method for solving differential equations we use, the permitted step-size becomes exceedingly small as τ increases. Thus practical considerations limit our results to $\tau \leq 4$ and to the requirement that the asymptotic solutions in the neighborhood of $\tilde{c} \sim 1$ be applied at $\tilde{c} = 0.95$ for both the first-order and perturbation solutions.

We take the case of $\tau = 4$, $\tilde{c}_o = 0.02$ and $c_{mo} = 0.833$ to be prototypical and show the results therefor in detail. In Fig. 5 the first-order solutions are given while Figs. 6 and 7 give the perturbation solutions associated with finite Reynolds and Damköhler numbers respectively. Again for the former we use the representative value, $C_1 = 1$. Note from Figs. 6 and 7 the dominance of the perturbed turbulent kinetic energy, i.e., of $\tilde{Q}_1$ and $\tilde{Q}_2$, over the other perturbation functions.

In Table 2 we present for a range of solutions the results for the eigenvalues and for parameters of interest based thereon. The first order eigenvalues, the coefficients a_{ij} and b_{ij} which permit the perturbed eigenvalues to be computed, and the physically significant quantities based on the perturbed eigenvalues are given. Again we shall discuss these results in detail in Section 6 but certain general remarks can be made here. As in the strong interaction case the magnitude of the perturbations associated with large but finite Reynolds numbers increase with heat release but decrease with corresponding values for Damköhler numbers. Moreover, the effect of the perturbations on turbulent flame speed are of opposite sign but on the ratio of turbulent kinetic energies are of the same sign. Finally, we note the weak dependence of the predicted behavior with $\tilde{c}_o$ and c_{mo}.

6. INTRODUCTION OF LAMINAR FLAME PARAMETERS AND COMPARISON WITH EXPERIMENT

As indicated earlier the behavior of turbulent flames is frequently correlated by experimentalists in terms of the characteristics of the classical laminar flame, determined either experimentally or theoretically, with the same chemical and thermodynamic situation as prevails for the turbulent flame in question. The implication from this practice is that one or both of our perturbation parameters are expressible in terms of laminar flame characteristics.

To pursue this implication further we consider the laminar flame speed, u_ℓ, and a measure of the laminar flame thickness, ℓ_ℓ; from [11, 12] we have

$$u_\ell = K_1 (\nu_o w_{max}/\rho_o)^{\frac{1}{2}} \tag{6.1}$$

$$\ell_\ell = K_2 (\nu_o \rho_o / w_{max})^{\frac{1}{2}} \tag{6.2}$$

where K_1 and K_2 are non-dimensional quantities given by the appropriate laminar flame solution. In the present context they should be treated as functions of the heat release parameter τ and as dependent on the chemical kinetic model representing w/w_{max}.

The quantities u_ℓ and ℓ_ℓ given by Eqs. (6.1) and (6.2) can be readily expressed in terms of our perturbation parameters; we find from the definitions of ϵ and δ

$$u_\ell^2 = \tilde{q}_o (K_1^2/aI_3)(\epsilon/\delta) \tag{6.3}$$

$$\ell_\ell^2 = \ell_o^2 (K_2^2 a^2 I_3)\, \epsilon\delta \tag{6.4}$$

Equation (6.3) indicates that u_ℓ is undefined in the first-order theory since $\epsilon, \delta = 0$ while Eq. (6.4) is consistent with the basic notion of the Bray-Moss model regarding a thin laminar flame provided both the turbulent Reynolds and Damköhler numbers are large.

Alternatively, Eqs. (6.3) and (6.4) yield

$$\epsilon = \left(\frac{\ell_\ell}{\ell_o}\right) \frac{u_\ell}{\tilde{q}_o^{\frac{1}{2}}} \frac{1}{K_1 K_2 a^{\frac{1}{2}}} \tag{6.5}$$

$$\delta = \left(\frac{\ell_\ell}{\ell_o}\right) \frac{\tilde{q}_o^{\frac{1}{2}}}{u_\ell} \frac{K_1}{K_2 I_3 a^{3/2}} \tag{6.6}$$

which show that our perturbation parameters are expressible in terms of the laminar flame characteristics.

Frequently only one of the two laminar flame characteristics introduced here are used by experimentalists to correlate their results; in this case only one of our perturbation parameters can be eliminated. We shall illustrate this in detail later.

Strong Interaction

In the case of strong interaction the orientation of the reaction zone is the predicted quantity most directly comparable with experiment.

From Eqs. (4.27)-(4.30) and (4.32) we find

$$\theta = \theta_o - \tfrac{1}{2} \frac{\tan\theta_o}{1+\tan^2\theta_o} \left(\left((a_{11}+a_{12}) + C_1(b_{11}+b_{12}) \right)\epsilon \right.$$

$$\left. + (b_{21}+b_{22})\mathcal{M}_o\delta + \ldots \right)$$

or for $\theta_o \ll 1$

$$\theta = \theta_o \left(1 - \tfrac{1}{2} \left((\ )\epsilon + (\ )\mathcal{M}_o\delta \right) + \ldots \right) \tag{6.7}$$

The results given in Table 1 can be used to evaluate the coefficients in Eq. (6.7).

The value of Φ has been selected as discussed in Appendix 3 so that the predictions of the first-order theory for θ_o are in good agreement with the results of Wright and Zukoski [2]. There are, however, no data permitting assessment of the perturbation effects. In this situation it may be useful to consider the counterpart for strong interaction of the correlation of the properties of normal flames given in [1]. Accordingly, we introduce the laminar flame speed and eliminate the Damköhler parameter; from Eq. (6.1) and the definition of $\mathcal{M}_o$ we have

$$\mathcal{M}_o\delta = \Phi \left(\frac{M_o}{I_3}\right) \frac{\tilde{q}_\infty}{u_\ell^2} K_1\epsilon$$

so that Eq. (6.7) becomes

$$\theta \cong \theta_o \left(1 - \tfrac{1}{2}\epsilon \left((a_{11} + a_{12}) + C_1 (b_{11} + b_{12}) \right.\right.$$

$$\left.\left. + (b_{21} + b_{22}) \frac{\Phi M_o K_1}{I_3} \frac{\tilde{q}_\infty^2}{u_\ell^2} \right) + \ldots \right) \qquad (6.8)$$

We eliminate the turbulent kinetic energy downstream of the flame from Eq. (6.8), since this is generally not measured. For this purpose only the first-order estimate of $\tilde{q}_\infty$ is needed; from the ratio $\tilde{u}_o / \tilde{q}_\infty^{\frac{1}{2}}$, the orientation of the flame and the resultant velocity upstream of the flame, V_o, we have for $\theta_o \ll 1$

$$\left(\frac{\tilde{q}_\infty^2}{u_\ell^2} \right)_o \cong \frac{\hat{\beta}_o \theta_o}{\Phi} \frac{V_o^2}{u_\ell^2} \qquad (6.9)$$

Thus Eq. (6.8) becomes

$$\theta = \theta_o \left(1 - \tfrac{1}{2}\epsilon \left((a_{11} + a_{12}) + C_1 (b_{11} + b_{12}) + (b_{21} + b_{22}) \right.\right.$$

$$\left.\left. \frac{M_o K_1 \hat{\beta}_o \theta_o^2}{I_3} \frac{V_o^2}{u_\ell^2} \right) + \ldots \right) \qquad (6.10)$$

In Appendix 2 we employ laminar flame theory to provide inter alia estimates for K_1 and for the quotient (M_o/I_3).* To illustrate the results given by Eq. (6.8) we take the exponent $n = 5$, $C_1 = 1$ and $\tau = 5$ and the results for our prototypical case $\tau = 5$, $\tilde{c}_o = 0.02$. With these values Eq. (6.8) yields

$$\theta \cong \theta_o \left(1 + \epsilon \left(11.7 - 1.02\,(10^{-2})\,(V_o^2/u_\ell^2) \right) + \ldots \right) \qquad (6.11)$$

From Eq. (6.11) we see that for values of the velocity ratio V_o/u_ℓ of 30-40, corresponding to values of $\tilde{u}_o/u_\ell$ of 3-4, the term arising from the replacement of the Damköhler perturbation is comparable to that due to the finite Reynolds number perturbation but of opposite sign so that the insensitivity of the angle of the flame observed by Wright and Zukoski [2] to a wide variety of conditions is perhaps explicable. For a fixed value of the ratio V_o/u_ℓ less than 34 a decrease in the turbulence Reynolds number leads to an increase in the angle of orientation; the opposite is true for values of the same velocity ratio

---

*It should be noted that two separate calculations of these quantities can be envisaged. The origin of K_1 via Eq. (6.1) implies that it is determined by the solution for the classical laminar flame; on the contrary, the quotient M_o/I_3 relates to the distribution f(c) within a laminar flame embedded in the turbulent reaction zone in question and thus in principle involves a separate calculation. For simplicity and consistency with the assumed insensitivity in the Bray-Moss model of the results to the details of f(c), we use the same solution for both calculations.

greater than 34. Note that in general the validity of the perturbation analysis may be questioned for $\epsilon \geq 10^{-2}$, i.e., for $R_T \leq 10^3$.

Normal Flames

In considering the implications of our perturbation analysis for normal flames we focus on the recent correlation of [1] which relates the ratio of turbulent to laminar flame speeds to the ratio of initial turbulent intensity to laminar flame speed for a wide range of experimental data and thus of turbulence Reynolds numbers. The absence in the correlation of heat release as a parameter implies that over the range of τ of practical interest, i.e., $4 \leq \tau \leq 9$, the variation of the ratios in question is within the scatter of the experimental results. Accordingly, we treat our results for $\tau = 4$ as being representative of our predictions over the entire range of τ of interest and compare these results with the data given in [1].

The present analysis can be recast to facilitate that comparison; Eqs. (5.1), (5.2), and (5.20)-(5.24) lead to

$$\frac{\tilde{u}_o}{u_\ell} = \left(\frac{\Phi}{\tilde{\beta}_o(1+\hat{Q}_o)}\right)^{\frac{1}{2}} \frac{\tilde{q}_o^{\frac{1}{2}}}{u_\ell} \left(1 - \tfrac{1}{2}\left(Q_{\infty o}(a_{12}+C_1 b_{12}) + (a_{11}+C_1 b_{11})\right)\epsilon - \tfrac{1}{2}(Q_\infty b_{22} + b_{21})\hat{M}\delta + \ldots\right) \tag{6.12}$$

Equation (6.12) leads to the anomalous result that as $\tilde{q}_o^{\frac{1}{2}}/u_\ell \sim 0$, $\tilde{u}_o/u_\ell \sim 0$; this pathological behavior is associated with the assumption of a high turbulence Reynolds number inherent in the Bray-Moss model and can be removed by heuristically replacing the left side of Eq. (6.12) and appropriate subsequent equations by $(\tilde{u}_o/u_\ell) - 1$.

Equation (6.12) with $\epsilon = \delta = 0$ and with the left side altered provides the basis on which the value of $\Phi = 1.4$ used here is selected in Appendix 3. To investigate the effect of Reynolds number given by Eq. (6.12) we eliminate $\hat{M}$ and introduce the laminar flame speed. From the definition of $\hat{M}$ and δ we find that

$$\hat{M}\delta = \Phi K_1^2 \left(\frac{M_o}{I_3}\right) \frac{1}{1+\hat{Q}_o} \left(\frac{\tilde{q}_o}{u_\ell^2}\right) \epsilon \tag{6.13}$$

so that Eq. (6.12) becomes

$$\frac{\tilde{u}_o}{u_\ell} - 1 = \left(\frac{\Phi}{\tilde{\beta}_o(1+\hat{Q}_o)}\right)^{\frac{1}{2}} \frac{\tilde{q}_o^{\frac{1}{2}}}{u_\ell} \left(1 - \tfrac{1}{2}\left(Q_{\infty o}(a_{12}+C_1 b_{12}) + (a_{11}+C_1 b_{11})\right.\right.$$

$$\left.\left. + (Q_{\infty o} b_{22} + b_{21}) \Phi K_1^2 \left(\frac{M_o}{I_3}\right) \frac{1}{1+\hat{Q}_o} \frac{\tilde{q}_o}{u_\ell^2} + \ldots\right)\right) \tag{6.14}$$

To evaluate the coefficients in Eq. (6.14) we use the results in Appendix 2 and of our protypical case for normal flames; thus we let: $\tau = 4$, $\tilde{c}_o = 0.02$, $\Phi = 1.4$, $C_1 = 1$, and $n = 5$. There results

$$\frac{\tilde{u}_o}{u_\ell} - 1 = 1.14 \frac{\tilde{q}_o^{\frac{1}{2}}}{u_\ell} \left(1 + (11.3 - 0.750 \frac{\tilde{q}_o}{u_\ell^2}) \epsilon + \ldots\right) \tag{6.15}$$

Equation (6.15) displays the same opposing effects as shown in Eq. (6.11) for the strong interaction case; thus, for $q_o^{\frac{1}{2}}/u_\ell$ less than 3.88 a decrease in turbulence Reynolds number increases the turbulent flame speed whereas for $q_o^{\frac{1}{2}}/u_\ell$ greater than 3.88 the opposite effect is predicted.

Figure 8 shows $\tilde{u}_o/u_\ell$ calculated from Eq. (6.15) for $\epsilon = 0$, 3 (10^{-3}) and 7 (10^{-3}). In the region $\tilde{q}_o^{\frac{1}{2}}/u_\ell < 3.88$, the increase in the ordinate resulting from these values of ϵ is too small to show in this figure. Consequently, the perturbation analysis predicts that, at a fixed turbulence Reynolds number, the ratio of turbulent to laminar flame speeds initially increases nearly linearly with increase in upstream turbulence intensity. At higher turbulence intensities the finite Reynolds number curves drop below this straight line. The curves for $\epsilon \neq 0$ in Fig. 8 are continued until the perturbation reaches 20%.

We note that the predictions of the theory similar to Eq. (6.15) but for different values of τ and of the exponent n in the laminar flame theory do not appear to differ significantly in a qualitative sense from those given here.

Figure 9 shows two sets of experimental data which approximately define two extremes in the correlation of Abdel-Gayed and Bradley [1]. The upper band is from [14] and the lower band from [15], both being interpreted in the manner of [1]. It has been assumed that the length scale ℓ_o in our turbulence Reynolds number R_T is the same as that used in [1] to define $R_\ell = u' \ell/\nu$, where u' is the root mean square of the x-wise velocity component. In converting from the abscissa

u_ℓ/u' of [1] it has been assumed that $\overline{\rho u''^2}/\bar{\rho}\tilde{q} = 0.3$ and that $R_T = R_\ell/0.3^{\frac{1}{2}}$. Thus $\epsilon = 0,\ 3\ (10^{-3})$ and $7\ (10^{-3})$ corresponds to $R_\ell \to \infty$ and $R_\ell = 2 \times 10^3,\ 8.8 \times 10^2$, respectively.

If the two sets of data are given equal weight then, superficially at least, a trend suggesting a reduction of turbulent flame speed at lower turbulence Reynolds numbers might be discerned, as proposed in [1]. Closer inspection of the data in Figure 9 argues however that no convincing Reynolds number trend is evident in the data of either [14] or [15], considered separately, despite the fact that each covers a significant Reynolds number range. There is clearly serious disagreement between data from these sources at comparable Reynolds numbers and the principal distinction would appear to relate to experimental configuration and technique. The emphasis of these remarks is not significantly changed if the other data from [1] is incorporated in Figure 9.

A comparison between the perturbation solutions and experiment is therefore not straightforward. If experimental data are chosen from a particular source such as [14], then the predicted trend with Reynolds number is not supported. The relatively narrow range of flame speeds within which the perturbation is valid is comparable to the scatter in the data [14]. On the other hand the trend predicted by the perturbation analysis agrees with that reported in [1]. It is important to note that the form of presentation of the experimental data adopted here is that

suggested most naturally by the present analysis and not that of Abdel-Gayed and Bradley [1]. Their abscissa, u_ℓ/u', is related to the inverse of that introduced in Fig. 9 and leads to curves of broadly hyperbolic character. In consequence, and in contrast to the present approach, attention is focussed on modest values of $\tilde{q}_o^{\frac{1}{2}}/u_\ell$.

The Influence of the Perturbations on the Structure of the Normal Flame

It is of interest to consider the influence of the perturbations on the structure of the turbulent reaction zone. To show this influence requires selection of a length scale model. For consistency we take $\tilde{q}^{\frac{1}{2}}\ell$ to be constant. In this case the x-coordinate is given by

$$\frac{x}{\ell_o} = a\left(\frac{J_o}{(\tilde{u}_o/\tilde{q}_o^{\frac{1}{2}})_o} - \epsilon\left(\frac{J_1}{(\tilde{u}_o/\tilde{q}_o^{\frac{1}{2}})_o} + \frac{(\tilde{u}_o/\tilde{q}_o^{\frac{1}{2}})_1}{(\tilde{u}_o/\tilde{q}_o^{\frac{1}{2}})_o^2} J_o\right)\right.$$

$$\left. - \delta\left(\frac{J_2}{(\tilde{u}_o/\tilde{q}_o^{\frac{1}{2}})_o} + \frac{(\tilde{u}_o/\tilde{q}_o^{\frac{1}{2}})_2}{(\tilde{u}_o/\tilde{q}_o^{\frac{1}{2}})_o^2} J_o\right) + \ldots\right) \qquad (6.16)$$

where

$$J_o = J_o(\tilde{c}) = \int_{\tilde{c}_o}^{\tilde{c}} \frac{d\tilde{c}}{(1+\tau\tilde{c})^{1+p} S_o}$$

$$J_i = J_i(\tilde{c}) = \int_{\tilde{c}_o}^{\tilde{c}} \frac{S_i\, d\tilde{c}}{(1+\tau\tilde{c})^{1+p} S_o^2}, \quad i = 1, 2$$

We see from Eq. (6.16) that the predicted spatial distributions within the reaction zone depend on both the perturbed eigenvalues via the ratios $(\tilde{u}_o/\tilde{q}_o^{\frac{1}{2}})_i$, i = 1, 2 and on the perturbed solutions themselves via $S_i(\tilde{c})$.

In the spirit of our earlier considerations we eliminate the Damköhler perturbation in favor of the laminar flame speed; there results

$$\frac{x}{\ell_o} = \frac{a}{(\tilde{u}_o/\tilde{q}_o^{\frac{1}{2}})_o}\left(J_o - \epsilon\left(J_1 + \frac{(\tilde{u}_o/\tilde{q}_o^{\frac{1}{2}})_1}{(\tilde{u}_o/\tilde{q}_o^{\frac{1}{2}})_o} J_o + K_1^2\left(\frac{\hat{M}_o}{I_3}\right)\frac{\tilde{q}_o}{u_\ell^2}\left(\frac{J_2}{\hat{M}_o} + \frac{(\tilde{u}_o/\tilde{q}_o^{\frac{1}{2}})_2}{(\tilde{u}_o/\tilde{q}_o^{\frac{1}{2}})_o \hat{M}_o} J_o\right) + \ldots\right)\right) \tag{6.17}$$

If we evaluate the coefficients in Eq. (6.17) on the basis of our prototypical case for normal flames, we find

$$\frac{x}{\ell_o} = 0.0791\left(J_o - \epsilon\left(J_1 + 11.2\,J_o + 0.556\,\frac{\tilde{q}_o}{u_\ell}\left(\frac{J_2}{\hat{M}_o} - 2.55\,J_o\right)\right) + \ldots\right) \tag{6.18}$$

We again see the competing effects of the Reynolds and Damköhler perturbations. In Fig. 10 we show the distribution of the mean product concentration according to the first-order theory and to Eq. (6.18) with $\tilde{q}_o^{\frac{1}{2}}/u_\ell = 10$ which corresponds to the limit of validity of the perturbation analysis for the assumed value of the perturbation parameter, $\epsilon = 3(10^{-3})$.

Several remarks regarding Fig. 10 are indicated. First note that the thickness of the reaction zone is on the order of the reference length scale ℓ_o; this is in accord with the results of I but we here explicitly incorporate density effects in the modelling and therefore have somewhat altered solutions. The effect of the combined Reynolds and Damköhler perturbations on the structure of the reaction zone tends to reduce the thickness for the particular value of the ratio $\tilde{q}_o^{\frac{1}{2}}/u_\ell$ selected. For smaller values of this ratio the predicted reaction zone would be thickened somewhat.

7. CONCLUDING REMARKS

Premixed turbulent combustion theory [5-8] has been extended to include effects of molecular transport and finite chemical reaction rates. The corresponding premixed laminar flame properties then arise quite naturally as parameters of the turbulent flame formulation, as already found in experiments. It is the first time that this has been demonstrated theoretically.

A perturbation analysis has been made, for large values of turbulence Reynolds number and Damköhler number, and applied to highly oblique confined flames, in the strong interaction limit, and to normal or unconfined oblique flames. Numerical solutions have been obtained using separate values of the important modelling parameter Φ for these two cases.

The strong interaction solution yields an expression (Eq. (6.11)) for the flame angle θ as a function of R_T and V_o/u_ℓ. It is observed that, in the range of validity of the perturbation, the perturbation terms arising from Da and R_T are of similar magnitude but opposite sign. The tendency for these terms to cancel each other is offered as a tentative explanation of the experimentally observed [2] insensitivity of the flame angle to large changes in the composition and temperature of the combustible mixture.

In the case of normal and unconfined oblique flames the turbulent flame speed in the form $\tilde{u}_o^{\frac{1}{2}}/u_\ell$ has been predicted as a function of turbulence intensity, $\tilde{q}_o^{\frac{1}{2}}/u_\ell$, and turbulence Reynolds number, R_T; see Eq. (6.15). These are essentially the same variables as those employed in an empirical correlation of experimental data by Abdel-Gayed and Bradley [1]. The perturbation solution predicts that the turbulent flame speed at finite R_T falls below the high Reynolds number limit by an amount which increases with increasing $\tilde{q}_o^{\frac{1}{2}}/u_\ell$ and with decreasing R_T. The analysis shows that this effect arises because of the finite reaction rate terms in the equation, rather than the molecular transport terms, whose direct influence on $\tilde{u}_o/u_\ell$ is negligible. Equation (6.15) then shows that the first-order approximation to the flame speed is valid so long as

$$R_T \gg 8.3\ \tilde{q}_o/u_\ell^2$$

Convincing support for the perturbation predictions for normal flames is not found in the experimental data. Individual experiments appear not to show a trend of $\tilde{u}_o/u_\ell$ variation with R_T although the scatter of data points is large. On the other hand the predicted trend agrees qualitatively with that found by Abdel-Gayed and Bradley [1] from their correlation of experimental data.

ACKNOWLEDGMENT

This research was supported in part by the Office of Naval Research under Contract N00014-75-C-1143, USN Purdue Subcontract No. 8960-8 as part of Project SQUID. Our international collaboration was facilitated by a grant from the Science Research Council of Great Britain. An oral presentation of this research was given at the International Colloquium on the Gas Dynamics of Explosions and Reactive Systems, Stockholm, August 1977.

REFERENCES

1. Abdel-Gayed, R. G. and Bradley, D., Dependence of turbulent burning velocity on turbulent Reynolds number and ratio of laminar burning velocity to R.M.S. turbulent velocity. Sixteenth Symposium (International) on Combustion. The Combustion Institute (1977), p. 1725.

2. Wright, F. H. and Zukoski, E. E., Flame spreading from bluff-body flameholders. Eighth Symposium (International) on Combustion. The Combustion Institute (1962), pp. 933-943.

3. Borghi, R. and Moreau, P., Turbulent combustion in a premixed flow. Acta Astronautica 4, pp. 321-341 (1977).

4. Pope, S. B., The probability approach to the modelling of turbulent reacting flows. Combustion anf Flame 27, 299-312 (1976).

5. Bray, K. N. C. and Moss, J. B., A unified statistical model of the premixed turbulent flame. University of Southampton AASU Report No. 335 (1974).

6. Bray, K. N. C. and Moss, J. B., A unified statistical model of the premixed turbulent flame. Acta Astronautica 4, pp. 291-319 (1977).

7. Bray, K. N. C. and Libby, P. A., Interaction effects in turbulent premixed flames. Phys. of Fluids 19, pp. 1687-1701 (1976).

8. Libby, P. A. and Bray, K. N. C., Variable density effects in premixed turbulent flames. AIAA J. 15, pp. 1186-1193 (1977).

9. Favre, A., Statistical equations of turbulent gases. In Problems of Hydrodynamics and Continuum Mechanics (Society for Industrial and Applied Mathematics, Philadelphia, 1969), pp. 231-

10. Batchelor, G., The Theory of Homogeneous Turbulence. Cambridge University Press, pp. 68-75, 1967.

11. Williams, F. A., Combustion Theory. Addison-Wesley, Reading, Mass., 1965, pp. 95-136.

12. Williams, F. A., Theory of combustion in laminar flows. Annual Review of Fluid Mechanics 3, pp. 171-188, 1971.

13. Spalding, D. B., One-dimensional laminar flame theory for temperature-explicit reaction rates. Combustion and Flame 1, 296-307 (1957).

14. Kozachenko, L. S. and Kuznetsou, I. L., Comb. Expl. Shock Waves 1, 22 (1965).

15. Petrov, E. A. and Talantov, A. V., Izv. Vyss. Uchebn. Zau. (Aviat. Tekn.) 3 (1959), Candin ARS Jl. 31, 408 (1961).

LIST OF FIGURES

10. The spatial distribution of mean product mass fraction:

——— first-order theory, — — — Eq. (6.18): $\epsilon = 0.003$,

$\tilde{q}_o^{\frac{1}{2}}/u_\ell = 10$

APPENDIX 1. The Behavior as $\tilde{c} \sim 1$

We consider the behavior of the first order and perturbations solutions in the neighborhood of $\tilde{c} = 1$, first for the case of strong interaction and subsequently for normal flames. If Eq. (4.12) is put in an approximate form appropriate for $\tilde{c} \sim 1$, $\tilde{Q}_o \sim 0$, it may be solved to yield

$$S_o = -\lambda(1 - \tilde{c}) \tag{A1.1}$$

where $\lambda = \frac{1}{2}\left(1 - \left(1 + 4\hat{\beta}_o/(1+\tau)^{2+m}\right)^{\frac{1}{2}}\right) < 0$. Next the right side of Eq. (4.13) can be similarly approximated so that with Eq. (A1.1) integration leads to

$$G_o = -\alpha\lambda(1 - \tilde{c})/(1 - \lambda) \tag{A1.2}$$

where $\alpha = \left(\left(\hat{\epsilon}\tau/(1+\tau)\right) - \tau^2 \kappa_o\right)$. Next Eqs. (A1.1) and (A1.2) permit Eq. (4.14) to be integrated so that

$$\tilde{Q}_o = -\alpha(1 - \tilde{c})/(1 - \lambda) \tag{A1.3}$$

Equations (A1) - (A3) applied at a value of $\tilde{c}$ in the neighborhood of $\tilde{c} = 1$ provide the boundary conditions for the first order solution and are employed in I and II. Note that these solutions are free of arbitrary constants, the parameters λ and α depending only on the eigenvalues $\hat{\beta}_o$ and κ_o. In the solution for S_o a second root of the secular equation for λ is discarded so that $S_o \sim 0$ as $\tilde{c} \sim 1$; furthermore, in the integrations leading to Eqs. (A1.2) and (A1.3) complementary solutions

which have unacceptable behavior as $\tilde{c} \sim 1$ must be suppressed, leaving the particular solutions as the only valid ones. Similar considerations arise with the perturbation solutions.

As a preliminary remark we recall that earlier we assumed the parameter R_o to be unity; in addition we note that the quantities $E_1(\tilde{c})$ and $E_2(\tilde{c})$ and the ratio $(\tilde{\nu}/\nu_o)$ will approach constant values as $\tilde{c} \sim 1$; we shall denote these values with the subscript ∞. Finally, the asymptotic solutions for the first order functions given by Eqs. (A1.1) - (A1.3) are used in the analysis of the asymptotic behavior of the perturbation solutions.

Equation (4.15) takes on the following form as $\tilde{c} \sim 1$:

$$\frac{dS_i}{d\tilde{c}} + \frac{1-\lambda}{\lambda} \frac{S_i}{1-\tilde{c}} = -(1-\lambda) K_i \qquad \text{(A1.4)}$$

where K_i

$$K_i = \frac{\hat{\beta}_i}{\hat{\beta}_o} - \delta_{i2} \frac{2(c_{mo}-1)}{2c_{mo}-1} \frac{1}{(1+\tau)^k} \mathcal{M}_o + \delta_{i1} C_1 \frac{\tilde{\nu}_\infty}{\nu_o}$$

$$- \delta_{i1} \frac{\lambda}{1-\lambda} \left(\frac{2E_{2\infty}}{2c_{mo}-1} - \frac{2(c_{mo}-1)}{2c_{mo}-1} E_{1\infty} \right)$$

We note that again the complementary solution must be suppressed; thus the solution to Eq. (A1.4) is

$$S_i = - \frac{\lambda(1 - \lambda)\, K_i (1 - \tilde{c})}{1 - 2\lambda} \tag{A1.5}$$

With S_i determined, the asymptotic approximation to Eq. (4.17) yields

$$\frac{dG_i}{d\tilde{c}} + \frac{1}{\lambda} \frac{G_i}{1 - \tilde{c}} = - \frac{\alpha K_i}{1 - 2\lambda} + \kappa_o \tau^2 \left(\frac{\kappa_i}{\kappa_o}\right) - \delta_{i1} \frac{\alpha\lambda}{1 - \lambda} (1 + \tau)^{2+p}$$

$$= L_i \tag{A1.6}$$

with the solution

$$G_i = \frac{\lambda L_i (1 - \tilde{c})}{1 - \lambda} \tag{A1.7}$$

Finally, a convenient form for the boundary conditions for the $\tilde{Q}_i$ functions is obtained by substitution of Eq. (4.18) into Eq. (4.17), by applying the approximations appropriate for $\tilde{c} \sim 1$, and by quadrature; the result is

$$\tilde{Q}_i = G_i + \kappa_o \tau^2 \left(\frac{\kappa_i}{\kappa_o}\right)(1 - \tilde{c}) + \delta_{i1} (1 + \tau)^{2+p} G_o \tag{A1.8}$$

Equations (A1.5), (A1.7), and (A1.8) applied at a value of $\tilde{c}$ in the neighborhood of $\tilde{c} = 1$ provide the appropriate boundary conditions to initiate an integration in the direction of $\tilde{c} = \tilde{c}_o$ for the strong interaction case.

Equations (A1.1)-(A1.3) apply for the first order equations for normal flames provided

$$\lambda = \tfrac{1}{2}\left(1 - \left(1 + 4\tilde{\beta}_o \hat{Q}_o/(1+\tau)^{2+m}\right)^{\frac{1}{2}}\right) \tag{A1.9}$$

$$\alpha = -\hat{\epsilon}\tau\hat{Q}_o/(1+\tau) \tag{A1.10}$$

In addition the solutions for the perturbation functions S_i and G_i given by Eqs. (A1.5) and (A1.7) are retained with

$$K_i = \frac{\tilde{\beta}_i}{\tilde{\beta}_o} + \frac{\hat{Q}_i}{\hat{Q}_o} - \delta_{i2}\,\frac{2(c_{mo}-1)}{2c_{mo}-1}\,\frac{\hat{Q}_o}{(1+\tau)^k}\,\hat{M} + \delta_{i1}C_1\,\frac{\tilde{\nu}_\infty}{\nu_o}$$

$$- \delta_{i1}\,\frac{\lambda}{1-\lambda}\left(\frac{2E_{2\infty}}{2c_{mo}-1} - \frac{2(c_{mo}-1)}{2c_{mo}-1}\,E_{1\infty}\right) \tag{A1.11}$$

$$L_i = -\frac{\alpha K_i}{1-2\lambda} + \frac{\hat{\epsilon}\tau\hat{Q}_o}{1+\tau}\left(\frac{\hat{Q}_i}{\hat{Q}_o}\right) - \delta_{i1}(1+\tau)^{2+p}\,\frac{\alpha\lambda}{1-\lambda} \tag{A1.12}$$

Finally, a relation for the $\tilde{Q}_i$ perturbations convenient for numerical analysis and completely analogous to Eq. (A1.8) is obtained from Eqs. (5.13) and (5.14) with approximations appropriate for $\tilde{c} \sim 1$, i.e.,

$$\tilde{Q}_i = G_i + \frac{\epsilon\tau\hat{Q}_o}{1+\tau}\left(\frac{\hat{Q}_i}{\hat{Q}_o}\right)(1-\tilde{c}) + \delta_{i1}(1+\tau)^{2+p}\,G_o \tag{A1.13}$$

We note that these results for the asymptotic behavior of the perturbation solutions as $\tilde{c} \sim 1$ for normal flames are consistent with

those for the strong interaction case if $\tilde{\beta}_o \hat{Q}_o \sim \hat{\beta}_o$, $\hat{Q}_o \sim -1$, $\kappa \sim 0$, $\hat{Q}_o \hat{M} \sim \mathcal{M}_o$, replacements which correspond to $\theta \sim 90^o$ and Q_∞ becoming indefinitely large.

APPENDIX 2. Determination of Perturbation Parameters by Laminar Flame Theory

In earlier studies, Bray and Moss [5, 6] evaluate the integrals

$$I_{k+3} = \int_0^1 c^k \frac{w(c)}{w_{max}} f(c)\, dc, \qquad k = 0,\ 1 \tag{A2.1}$$

which arise in the closure of the chemical source term, on an ad hoc basis. The burning mode pdf, f(c), is taken to be a simple battlement shape, broadly characteristic of a laminar premixed flame, while the reaction rate employs an Arrhenius form. The requirements of the perturbation analysis for similar information are greater and invite a more rational approach.

The species balance equation for c *in a one-dimensional laminar* flame may be written in the form

$$\rho u \frac{dc}{dx} - \frac{d}{dx}\left(\rho D \frac{dc}{dx}\right) = w(c) \tag{A2.2}$$

while continuity assumes the form

$$\rho u = \dot{m} = \text{constant} \tag{A2.3}$$

If we assume the Schmidt Number to be unity and introduce the simplifying thermodynamic description of Section 2, then

$$\mu = \rho D = \mu_o (1 + \tau c) \tag{A2.4}$$

whence Eq. (A2.2) becomes

$$\dot{m} \frac{dc}{dx} - \frac{d}{dx} \left\{ \mu_o (1 + \tau c) \frac{dc}{dx} \right\} = w(c) \qquad \text{(A2.5)}$$

If we introduce

$$S \equiv \mu_o \frac{(1 + \tau c)}{\dot{m}} \frac{dc}{dx} \qquad \text{(A2.6)}$$

and treat c as the independent variable, then Eq. (A2.6) may be written as

$$S\left(1 - \frac{dS}{dc}\right) = \frac{\mu_o}{\dot{m}^2} (1 + \tau c)\, w(c) \qquad \text{(A2.7)}$$

Following Bray and Moss [5, 6], we have

$$f(c) = \left(\frac{dc}{dx} \int_0^1 \frac{dc}{(dc/dx)} \right)^{-1} \qquad \text{(A2.8)}$$

or, from Eq. (A2.6),

$$f(c) = \frac{1 + \tau c}{S \int_0^1 \left((1 + \tau c)/S \right) dc} \qquad \text{(A2.9)}$$

We note that the integrals indicated in Eqs. (A2.8) and (A2.9) have been implicitly taken to be convergent. In general this is not the case and a concept analogous to that used in experimental turbulence, namely gating, must be introduced. The consequence is that $f(c)$ is defined only for the range $\epsilon_g \leq c \leq 1 - \epsilon_g$ where $0 < \epsilon_g << 1$; entries for $0 \leq c \leq \epsilon_g$

and for $1 - \epsilon_g \leq c \leq 1$ are attributed to the Dirac delta functions at $c = 0, 1$. However, we shall see that when $f(c)$ is used in evaluating the various integrals of interest, the integrals are convergent, the integral in the denominator of Eq. (A2.9) is inessential, and ϵ_g can be allowed to vanish. Accordingly, the determination of $S(c)$ for a specified reaction rate expression, $w(c)$, permits an entirely self-consistent determination of the moments I_k and of other quantities required in the perturbation analysis.

Spalding [14] identifies certain reaction rate expressions which are both plausible and permit analytical solution of Eq. (A2.7) subject to the appropriate boundary conditions. It is thus convenient and sufficient for present purposes to let

$$w(c) = \alpha w_{max} c^n (1 - c^{n-1})/(1 + \tau c), \quad n \geq 2 \tag{A2.10}$$

where α is a numerical constant introduced to normalize $w(c)/w_{max}$. Then Eq. (A2.7) may be recast as

$$S(1 - \frac{dS}{dc}) = \lambda c^n (1 - c^{n-1}) \tag{A2.11}$$

where $\lambda \equiv (\alpha \mu_o w_{max}/\dot{m}^2)$ is the eigenvalue, reconciling the first order equation with the two boundary conditions

$$S(0) = S(1) = 0. \tag{A2.12}$$

By inspection the solution is found to be especially simple, namely

$$S = c(1 - c^{n-1})$$

$$\lambda = n \tag{A2.13}$$

so that Eq. (A2.9) becomes

$$f(c) = \frac{1 + \tau c}{c(1 - c^{n-1}) \int_{\epsilon_g}^{1-\epsilon_g} (1 + \tau c) \left(c (1 - c^{n-1})\right)^{-1} dc},$$

$$\epsilon_g \leq c \leq 1 - \epsilon_g \tag{A2.14}$$

where we explicitly introduce the gating parameter, ϵ_g.

We now use these solutions to obtain with $\epsilon_g \sim 0$ the parameters

$$c_{mo} = \frac{\int_0^1 c^{n+1} dc}{\int_0^1 c^n dc} = \frac{n}{n+1} \tag{A2.15}$$

and

$$\frac{M_o}{I_3} = \frac{n}{\alpha} \int_0^1 \left(\frac{1 - c}{1 - c^{n-1}}\right) dc \tag{A2.16}$$

Note that c_{mo} is independent of τ but that (M_o/I_3) does depend on τ via α. In general a numerical evaluation of Eq. (A2.16) is required. In addition the parameters K_1 and K_2 arising in Section 6

can be evaluated. First, by comparison of the definitions of u_ℓ, and λ (cf. Eqs. (6.1) and (A2.11)) we find

$$K_1^2 = \alpha/n \tag{A2.17}$$

Next, if we define $\ell_\ell = 1/(dc/dx)_{max}$, Eqs. (6.2) and (A2.6) lead to

$$K_2 = \left(\frac{n}{\alpha}\right)^{\frac{1}{2}} \left(\frac{1 + \tau c}{S}\right)_{max}$$

$$= \left(\frac{n}{\alpha}\right) \left(\frac{1 + \tau c}{c(1 - c^{n-1})}\right)_{max} \tag{A2.18}$$

We show in Table 3 the values of the various parameters of interest for ranges of τ and for $n = 3$ and 5, values considered representative.

APPENDIX 3. Numerical Values of Φ

The parameter

$$\Phi = \frac{a C \ell_1}{(2c_{mo} - 1)\ell_2} \tag{A3.1}$$

must be specified before the perturbation solutions can be calculated and before comparison with experiment can be carried out. In the strong interaction case, Φ is estimated from the experiments of Wright and Zukoski [2] by matching the measured flame angle to that predicted by the first-order solution. The relevant equation is (see Eq. (4.1), (4.2))

$$\tan^2 \theta_o = \frac{\Phi}{\hat{\beta}_o \kappa_o} \tag{A3.2}$$

If we use our prototypical case for strong interaction to select a value for Φ, we find with $\hat{\beta}_o = 87.2$, $\kappa_o = 0.0897$ and $\Phi = 0.1$ that $\theta_o = 6.45^o$ in satisfactory agreement with [2]. Accordingly, we adopted this value of Φ for all calculations of the limiting case of strong interaction.

For normal flames and unconfined oblique flames, Φ is estimated from the experimental data of [14]. Using the first-order solution, we obtain Φ from Eq. (6.12) as

$$\frac{\tilde{u}_o}{u_\ell} - 1 = \left[\frac{\Phi}{\tilde{\beta}_o(1 + Q_o)}\right]^{\frac{1}{2}} \frac{\tilde{q}_o^{\frac{1}{2}}}{u_\ell} \tag{A3.3}$$

With $\tilde{\beta}_o = 0.413$ and $\hat{Q}_o = 1.62$, it is found that $\Phi = 1.4$. In Fig. 9, the line $\epsilon = 0$, representing the first-order solution with $\Phi = 1.4$, is seen to compare well with experimental data from [14].

It is evident from (A3.1) that the parameter Φ incorporates uncertain features of both the thermochemical and fluid mechanical modelling. The significantly different values of Φ necessary to admit quantitative comparison in both the unconfined and strong interaction cases suggest major differences, either in local structure, f(c) (and hence c_m), or in the "universal" parameters, for example. On the other hand, in the light of earlier discussions, the experimental data are also not without ambiguity. Further investigation is indicated.

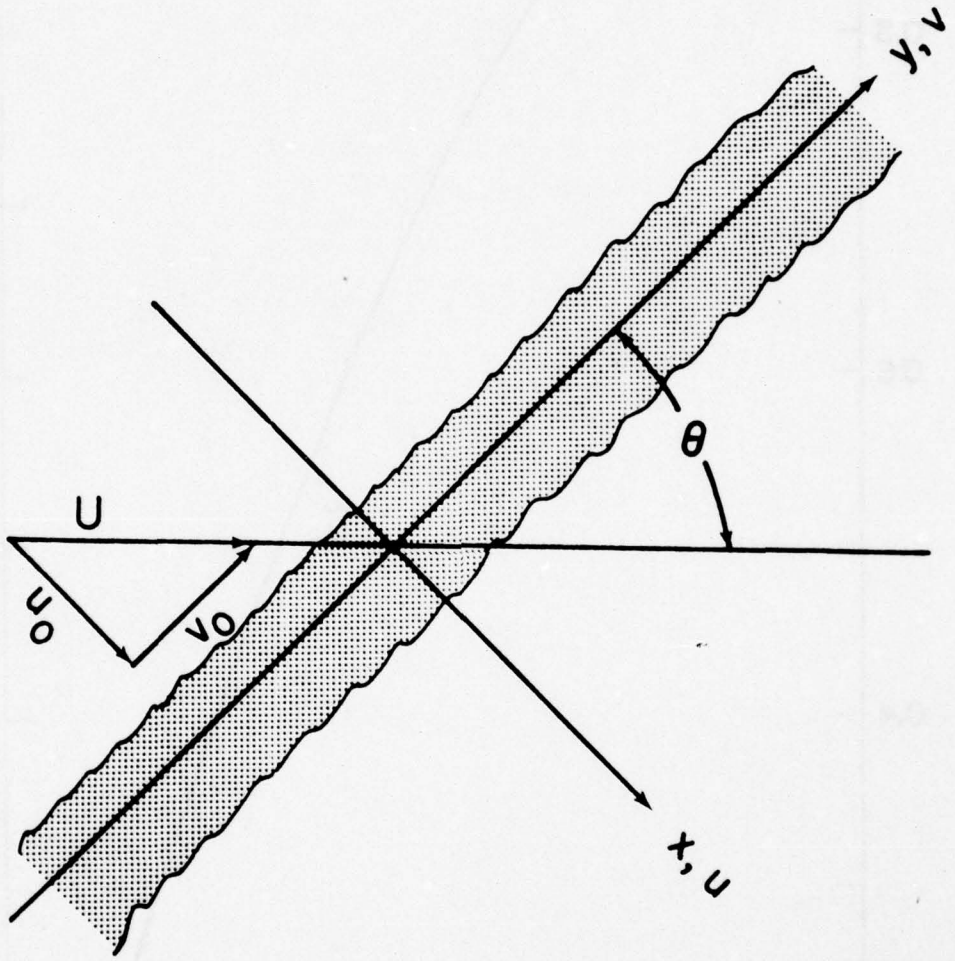
y, v
θ
U
U_0
V_0
x, u

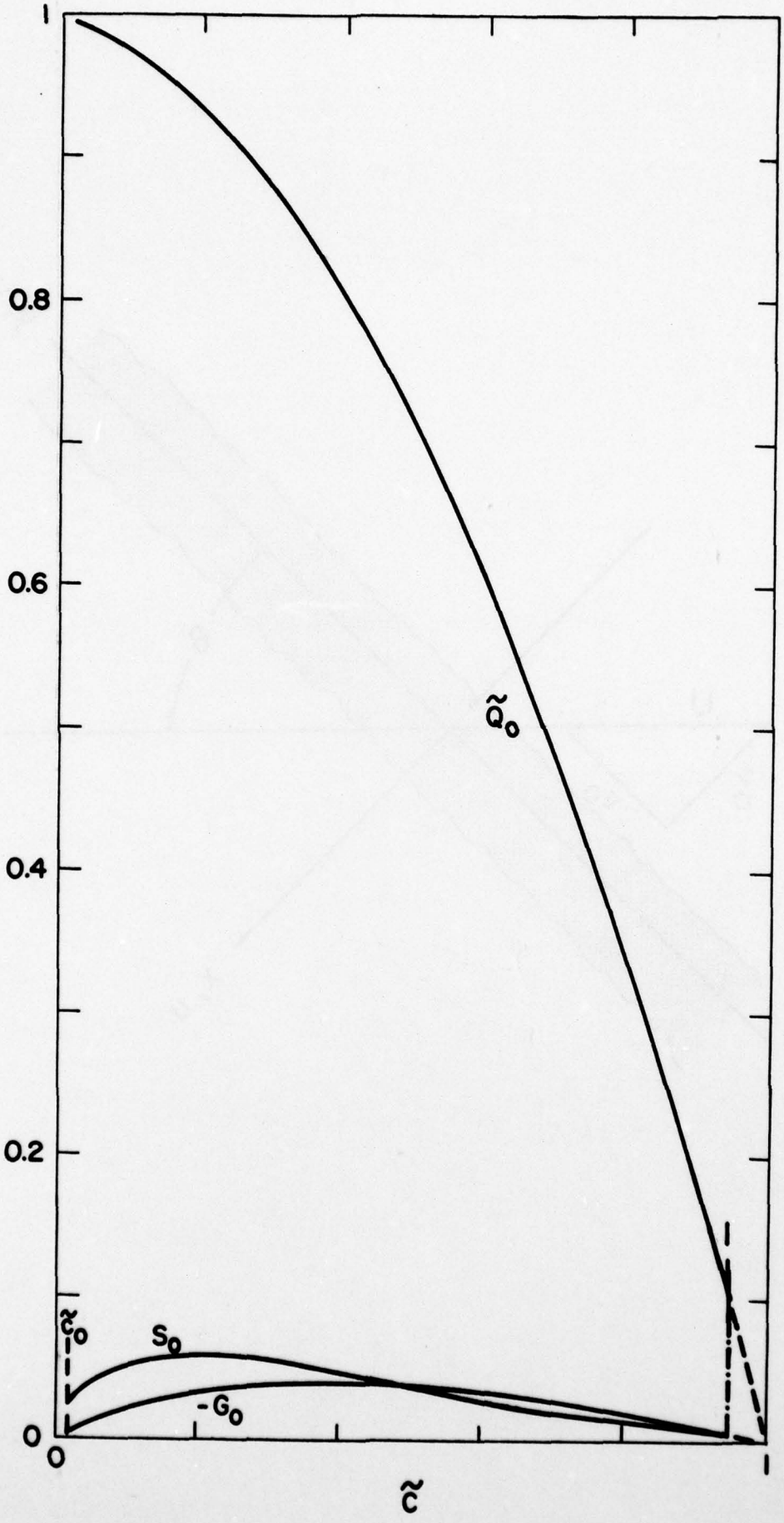
1
0.8
0.6
0.4
0.2
0
0
$\tilde{Q}_o$
$\tilde{\tau}_o$
S_o
$-G_o$
$\tilde{c}$

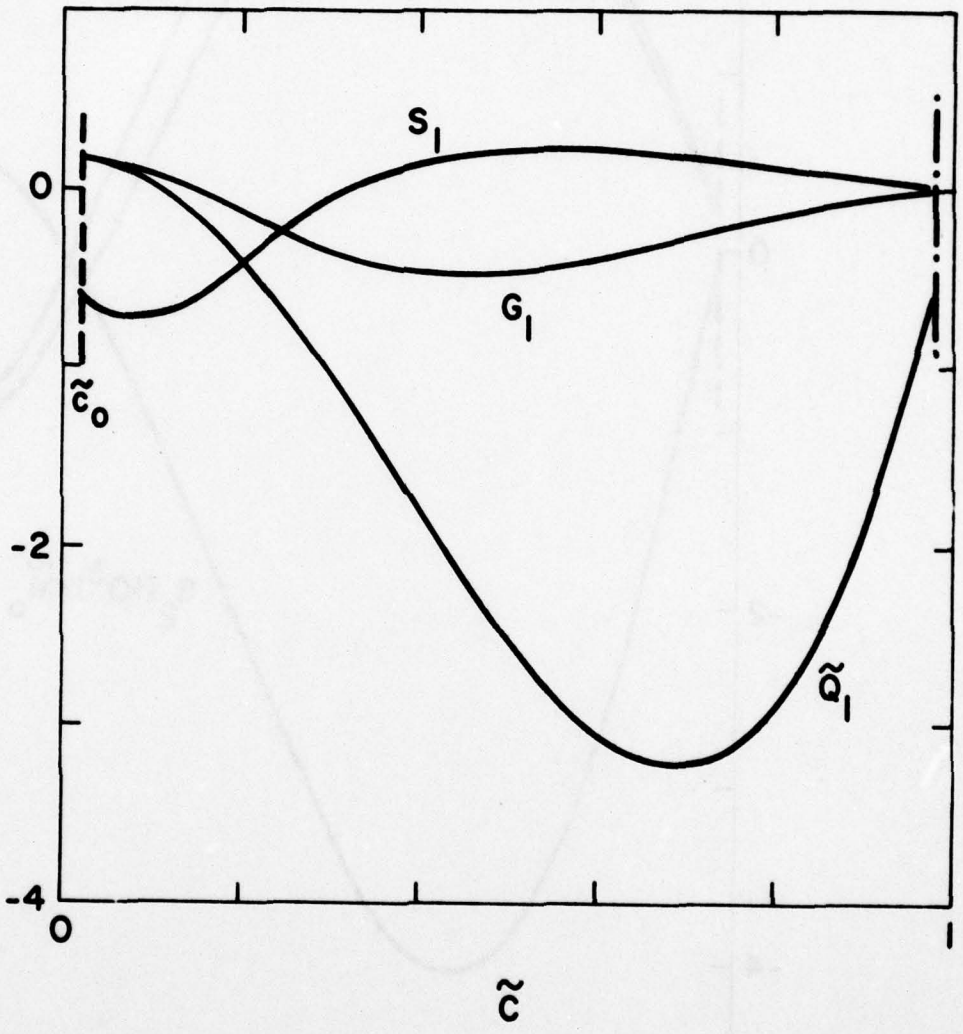
S_1
G_1
$\tilde{Q}_1$
$\tilde{c}_0$
0
-2
-4
0
1
$\tilde{c}$

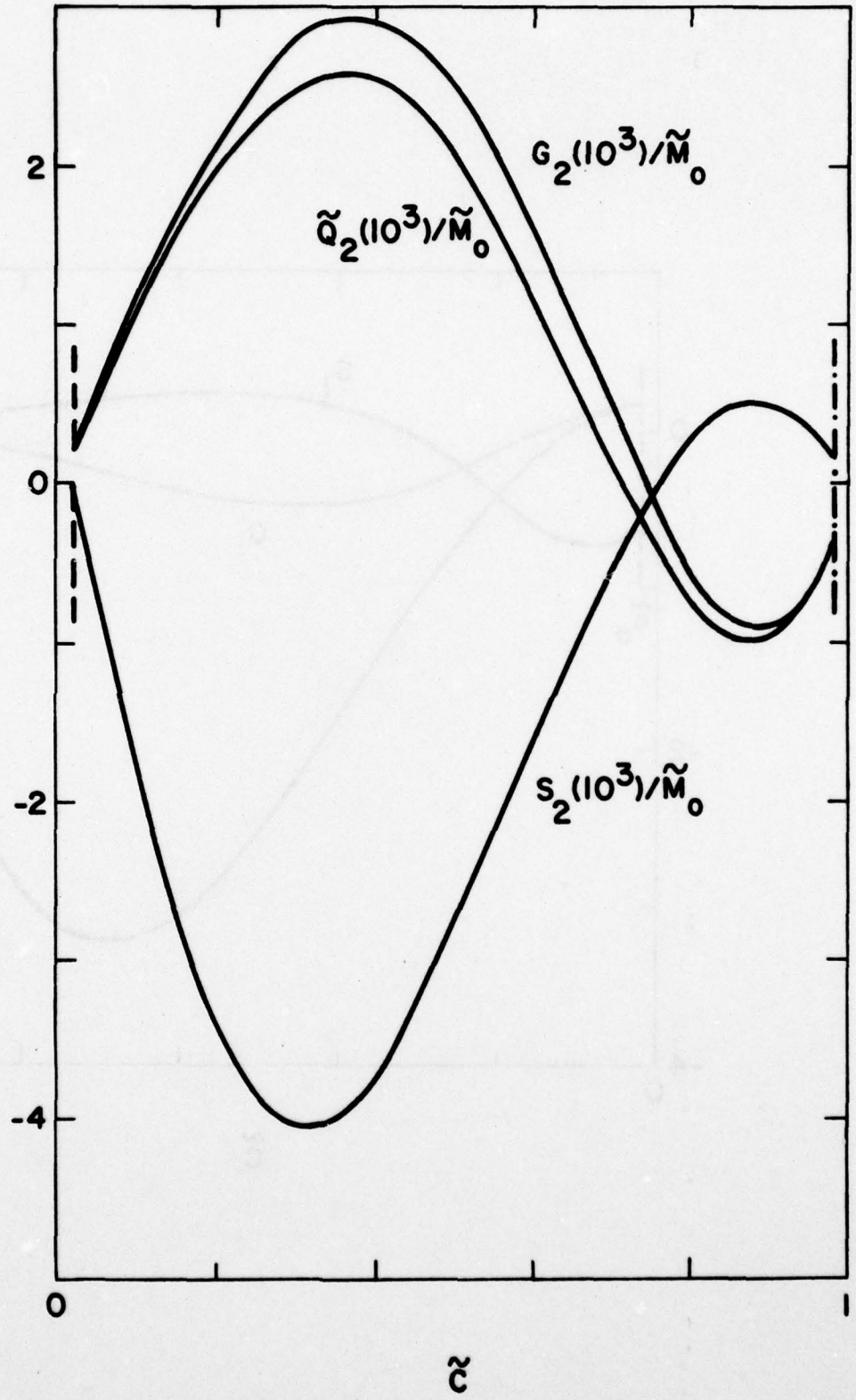
2
0
-2
-4
0
1
$G_2(10^3)/\tilde{M}_0$
$\tilde{Q}_2(10^3)/\tilde{M}_0$
$S_2(10^3)/\tilde{M}_0$
$\tilde{c}$

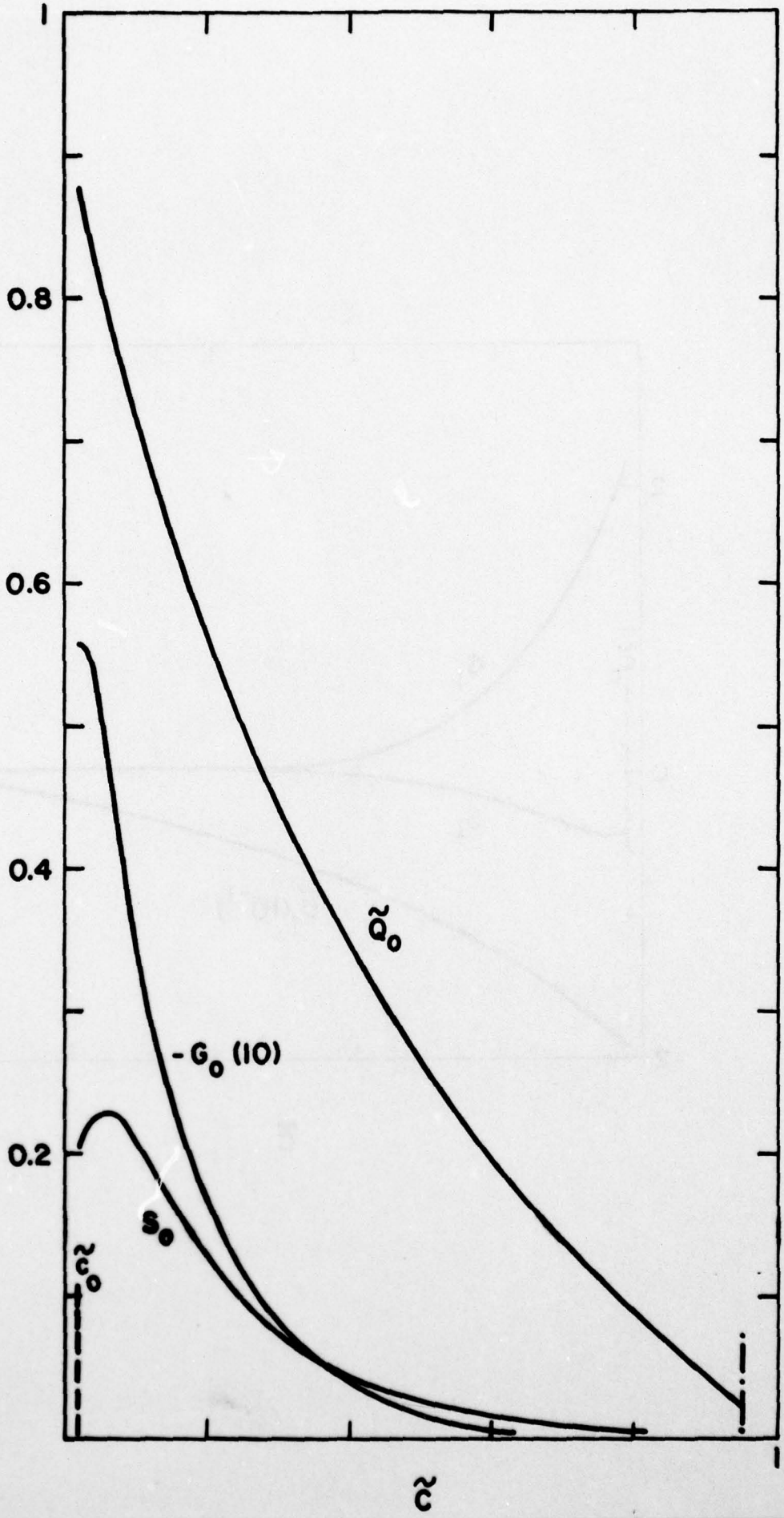
1
0.8
0.6
0.4
0.2
$\tilde{Q}_0$
$-G_0(10)$
S_0
$\tilde{c}_0$
$\tilde{c}$

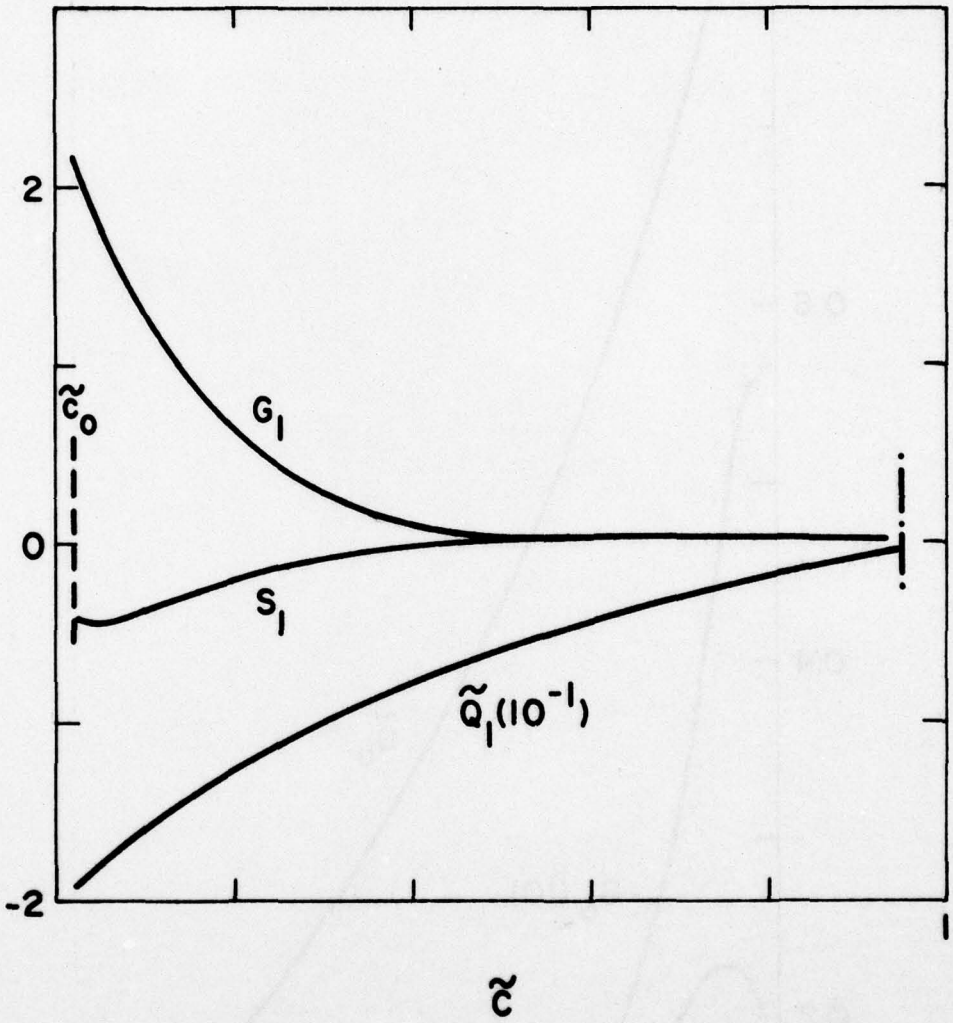
2
0
-2
1
$\tilde{c}_0$
G_1
S_1
$\tilde{Q}_1(10^{-1})$
$\tilde{c}$

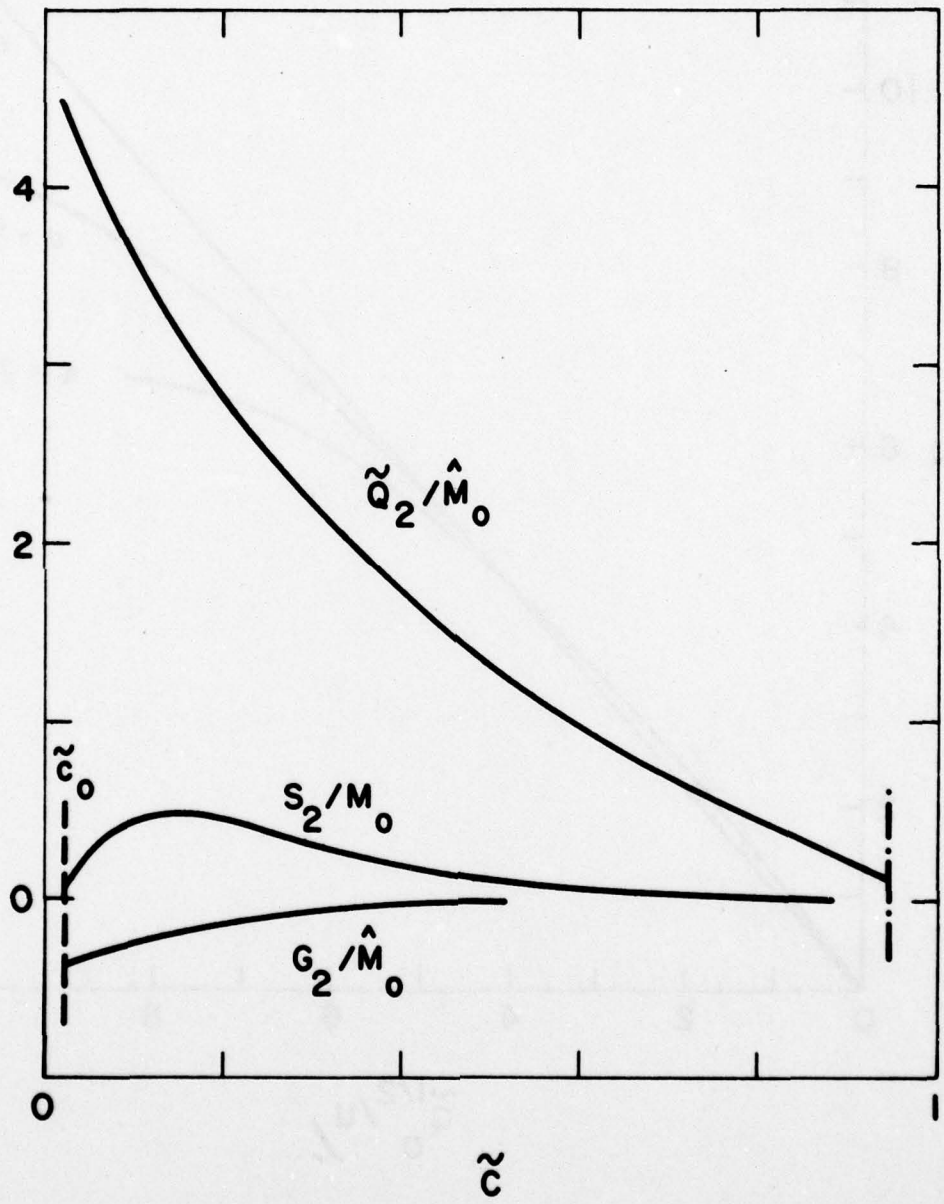
4
2
0
0
1
$\tilde{Q}_2/\hat{M}_0$
$\tilde{c}_0$
S_2/M_0
$G_2/\hat{M}_0$
$\tilde{c}$

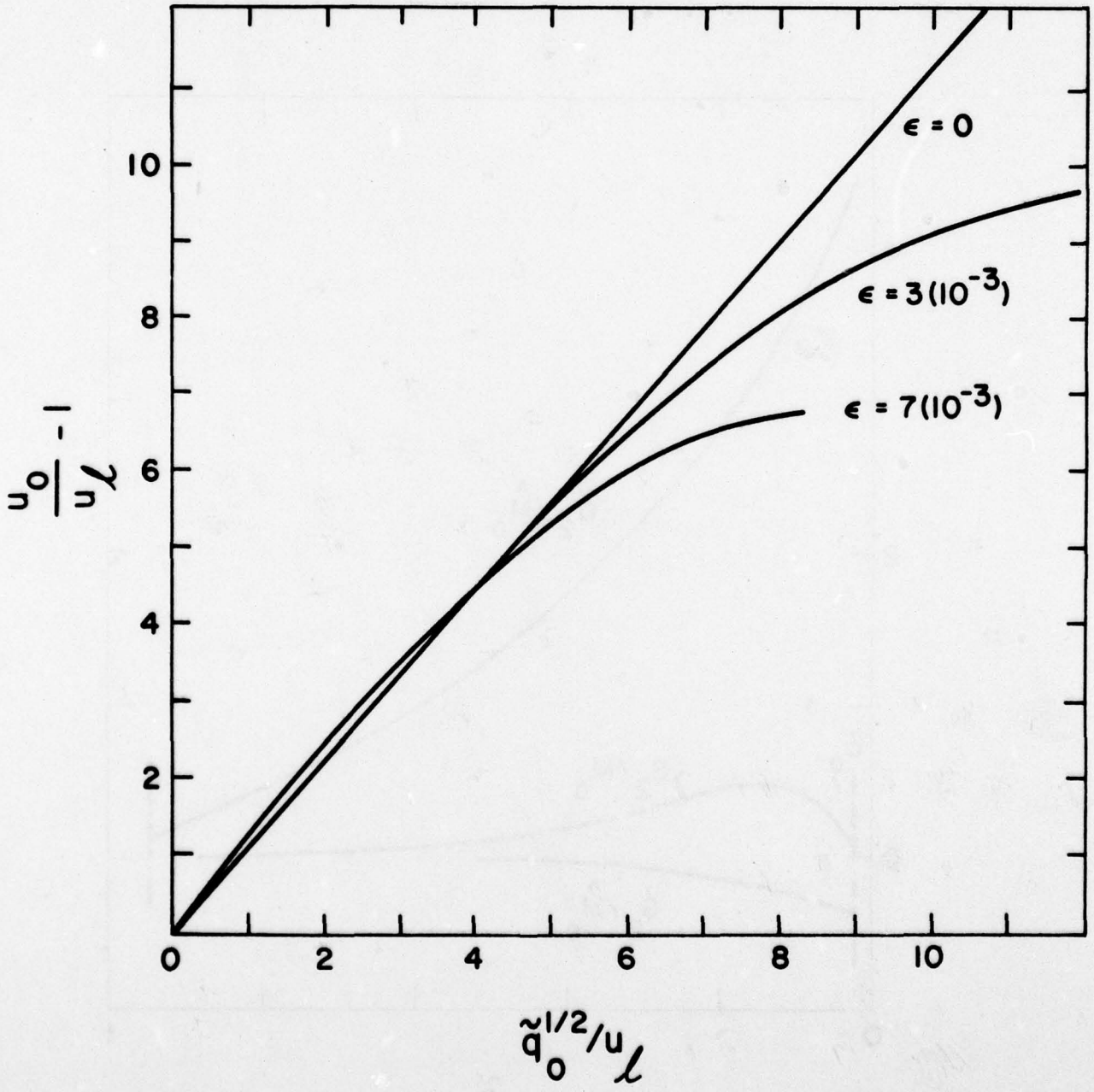
$\epsilon = 0$
$\epsilon = 3(10^{-3})$
$\epsilon = 7(10^{-3})$
$\frac{u_0}{u_\ell} - 1$
$\tilde{q}_0^{1/2}/u_\ell$
0
2
4
6
8
10

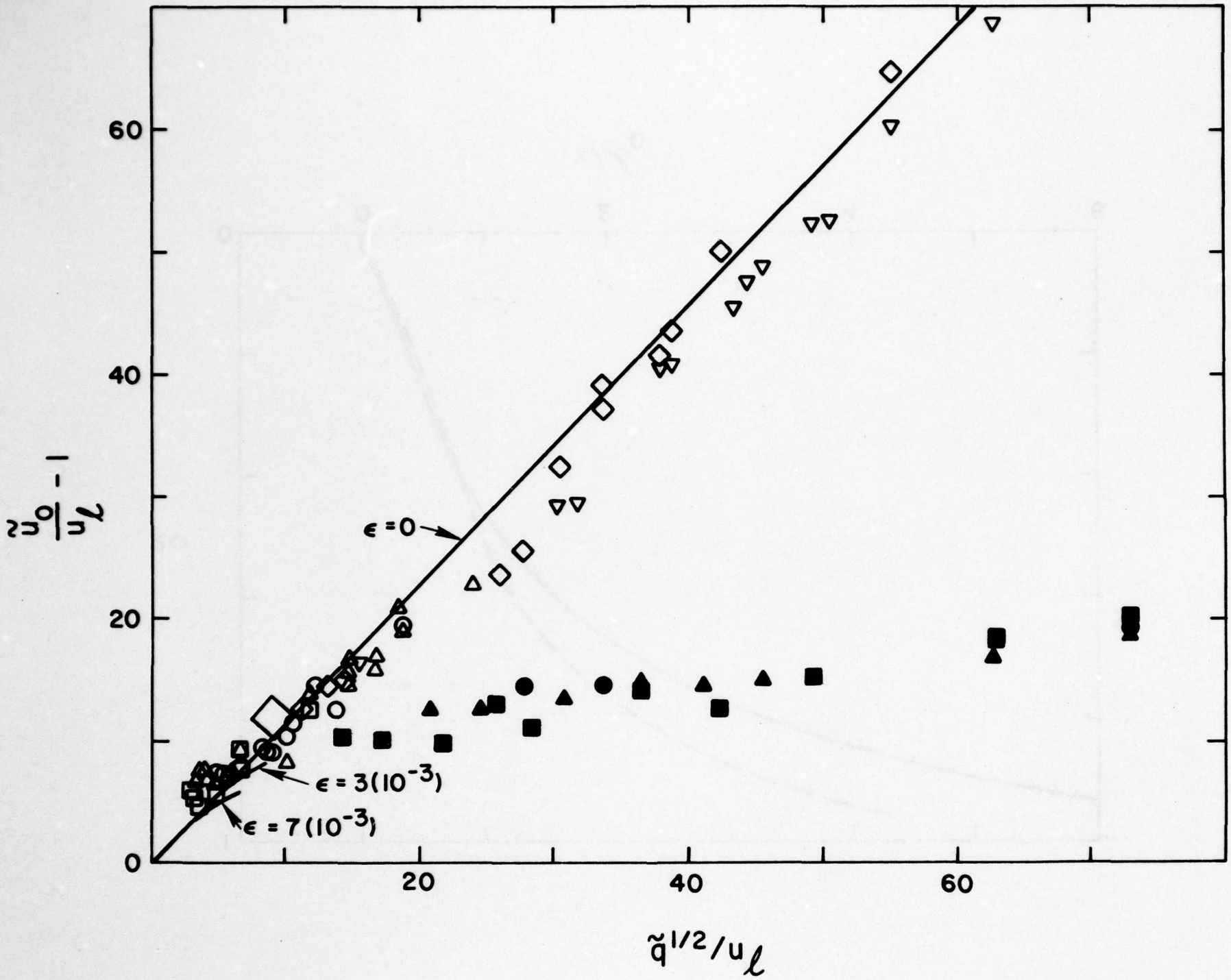
60
40
20
0
20
40
60
$\tilde{\eta}^{-1}/u_\ell$
$\tilde{q}^{1/2}/u_\ell$
$\epsilon = 0$
$\epsilon = 3(10^{-3})$
$\epsilon = 7(10^{-3})$

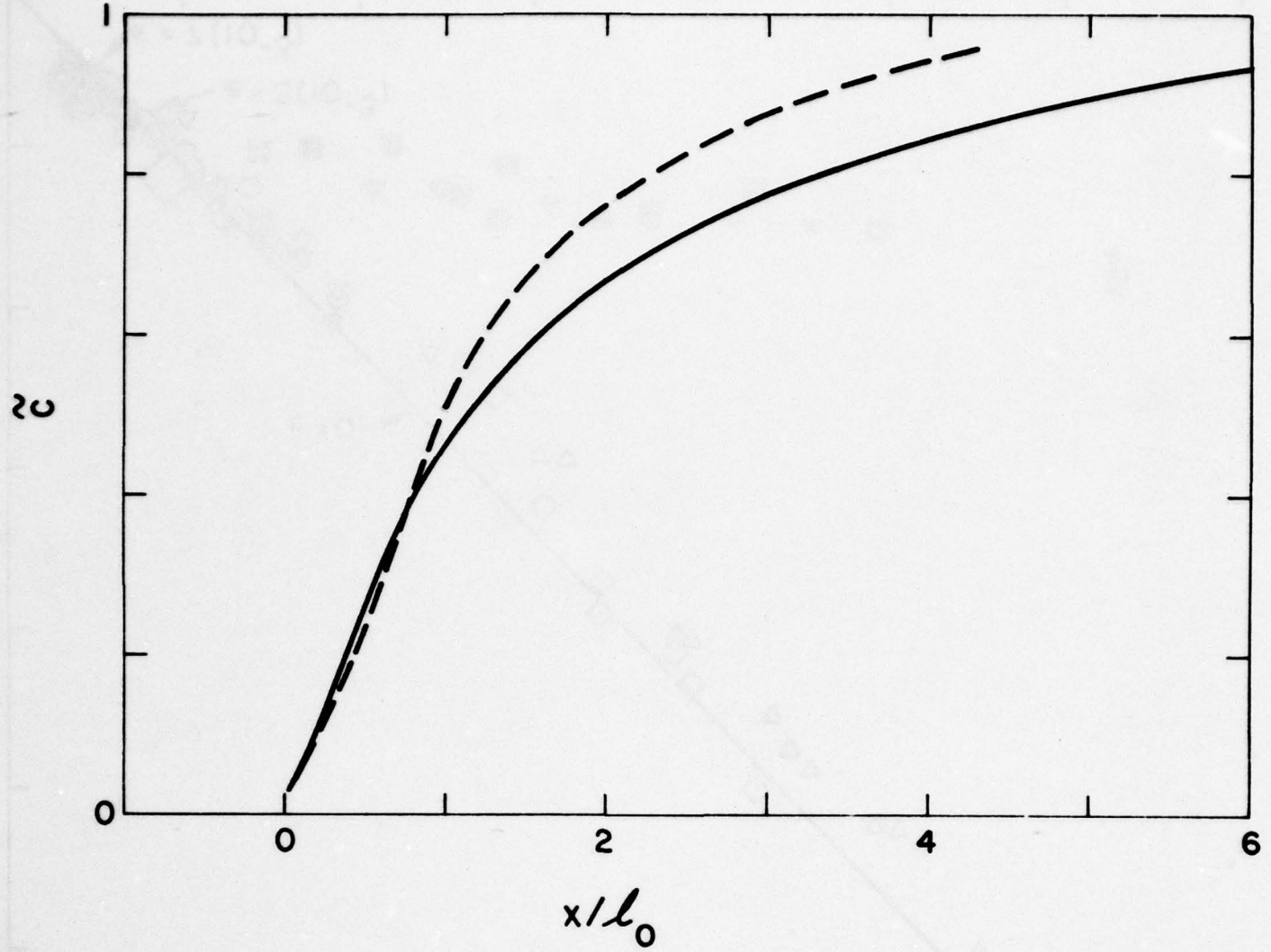
1
0
0
2
4
6
x/l0

Table 1. Results Relative to the Eigenvalues for Strong Interaction

τ	$\tilde{c}_o$	c_{mo}	$\hat{\beta}_o$	$\kappa_o(10)$	$(\tilde{u}_o/\tilde{q}_\infty^{\frac{1}{2}})_o(10)$	ϑ_o^o	a_{11}	b_{11}	a_{12}	b_{12}	$b_{21}(10)$	$b_{22}(10^3)$	$\frac{(\tilde{u}_o/\tilde{q}_\infty^{\frac{1}{2}})_o}{(\tilde{u}_o/\tilde{q}_\infty^{\frac{1}{2}})_1}$	θ_1/θ_o	$\frac{(\tilde{u}_o/\tilde{q}_\infty^{\frac{1}{2}})_2}{(\tilde{u}_o/\tilde{q}_\infty^{\frac{1}{2}})_o m_o}(10^3)$	$\theta_2/\theta_o m_o(10)$
5	0.02	0.833	87.2	0.897	0.339	6.45	-16.5	-7.51	0.481	0.116	0.744	-0.557	12.0	11.7	-0.372	-0.369
	0.01		85.6	0.897	0.342	6.51	-15.6	-7.38	0.480	0.115	0.724	-0.566	11.5	11.2	-0.362	-0.359
	0.04		93.2	0.898	0.328	6.24	-18.9	-8.00	0.482	0.120	0.814	-0.520	13.5	13.1	-0.407	-0.404
	0.02	0.750	87.2	0.897	0.339	6.45	-16.4	-7.51	0.493	0.116	0.886	-0.564	12.0	11.7	-0.443	-0.440
4	0.02	0.833	59.1	1.40	0.411	6.28	-12.1	-6.14	0.335	0.0932	0.988	-0.696	9.12	8.91	-0.494	-0.491
3	0.02		36.7	2.47	0.522	6.00	-8.48	-4.79	0.202	0.0673	1.38	-0.849	6.64	6.50	-0.691	-0.686

Table 2. Results Relative to the Eigenvalues for Normal Flames

τ	$\tilde{c}_o$	c_{mo}	$\tilde{\beta}_o$	$\hat{Q}_o$	$\tilde{u}_o/\tilde{q}_o^{\frac{1}{2}}$	$Q_{\infty o}$	a_{11}	b_{11}	a_{12}	$b_{12}(10)$	b_{21}	$b_{22}(10)$	$\frac{(\tilde{u}_o/\tilde{q}_o^{\frac{1}{2}})_1}{(\tilde{u}_o/\tilde{q}_o^{\frac{1}{2}})_o}$	$Q_{\infty 1}/Q_{\infty o}(10)$	$\frac{(\tilde{u}_o/\tilde{q}_o^{\frac{1}{2}})_2}{(\tilde{u}_o/\tilde{q}_o^{\frac{1}{2}})_o \hat{M}_o}$	$Q_{\infty 2}/Q_{\infty o}\hat{M}_o(10^2)$
4	0.02	0.833	0.413	1.62	1.14	0.618	-20.6	-2.06	0.242	0.190	5.10	0.170	11.2	0.997	-2.56	0.649
	0.04		0.748	1.61	0.847	0.617	-21.4	-2.73	0.677	0.247	4.25	0.179	11.9	2.30	-2.13	0.686
	0.02	0.75	0.413	1.62	1.14	0.618	-19.9	-2.06	0.249	0.190	6.10	0.213	10.9	1.02	-3.06	0.814
3	0.02	0.833	0.309	1.95	1.24	0.661	-12.8	-1.72	0.157	0.138	5.98	0.195	5.48	0.579	-3.00	0.661
2	0.02		0.210	2.58	1.36	0.721	-7.14	-1.44	0.0901	0.0912	7.58	0.241	4.25	0.279	-3.80	0.672
1	0.02		0.111	4.35	1.54	0.813	-3.42	-1.21	0.0365	0.0429	14.2	0.440	2.30	0.0763	-7.12	0.823

Table 3. Parameters Given by Laminar Flame Theory

n	c_{mo}	τ	M_o/I_3	K_1	K_2
3	0.750	0	0.376	1.34	1.94
		1	0.213	1.78	2.25
		2	0.149	2.12	2.50
		3	0.115	2.42	2.70
		4	0.0937	2.68	2.89
		5	0.0790	2.92	3.05
		6	0.0683	3.14	3.21
		7	0.0602	3.35	3.35
		8	0.0538	3.54	3.49
		9	0.0486	3.72	3.63
5	0.833	0	0.600	0.969	1.93
		1	0.323	1.32	2.32
		2	0.231	1.59	2.64
		3	0.168	1.83	2.90
		4	0.135	2.02	3.15
		5	0.113	2.22	3.36
		6	0.0930	2.40	3.56
		7	0.0859	2.56	3.75
		8	0.0766	2.71	3.93
		9	0.0691	2.85	4.10

SECURITY CLASSIFICATION OF THIS PAGE *(When Data Entered)*

REPORT DOCUMENTATION PAGE

READ INSTRUCTIONS BEFORE COMPLETING FORM

1. REPORT NUMBER: SQUID — UCSD-10-PU
2. GOVT ACCESSION NO.
3. RECIPIENT'S CATALOG NUMBER

4. TITLE (and Subtitle): EFFECTS OF FINITE REACTION RATE AND MOLECULAR TRANSPORT IN PREMIXED TURBULENT COMBUSTION.

5. TYPE OF REPORT & PERIOD COVERED: Technical-Scientific rept.
6. PERFORMING ORG. REPORT NUMBER

7. AUTHOR(s): Paul A. Libby, K.N.C. Bray and J.B. Moss

8. CONTRACT OR GRANT NUMBER(s): N00014-75-C-1143

9. PERFORMING ORGANIZATION NAME AND ADDRESS
University of California-San Diego
La Jolla, California

10. PROGRAM ELEMENT, PROJECT, TASK AREA & WORK UNIT NUMBERS: NR-098-038

11. CONTROLLING OFFICE NAME AND ADDRESS
Project SQUID Headquarters
Chaffee Hall
Purdue University, West Lafayette, Ind. 47907

12. REPORT DATE: May 1978
13. NUMBER OF PAGES: 82 (12 85p.)

14. MONITORING AGENCY NAME & ADDRESS *(if different from Controlling Office)*
Office of Naval Research, Power Program, Code 473
Department of the Navy
800 No. Quincy Street
Arlington, VA 22217

15. SECURITY CLASS. *(of this report)*: Unclassified

15a. DECLASSIFICATION/DOWNGRADING SCHEDULE

16. DISTRIBUTION STATEMENT *(of this Report)*
This document has been approved for public release and sale; its distribution is unlimited.

17. DISTRIBUTION STATEMENT *(of the abstract entered in Block 20, if different from Report)*
Same

18. SUPPLEMENTARY NOTES

19. KEY WORDS *(Continue on reverse side if necessary and identify by block number)*
Premixed combustion
Turbulent combustion
Finite reaction rate
Molecular transport

20. ABSTRACT *(Continue on reverse side if necessary and identify by block number)*
Previous application of the Bray-Moss model for premixed turbulent combustion to planar, oblique and normal flames is extended to include the effect of large but finite values of the two dominant characteristic numbers, a turbulence Reynolds number providing a measure of the intensity of the turbulence and a Damkohler number relating a turbulence time to a chemical time. A classical perturbation analysis involving two small parameters proportional to the inverse of these two numbers is carried out to account separately for the effects of molecular transport and of altered scalar dissipation and for → next page

DD FORM 1 JAN 73 1473 EDITION OF 1 NOV 65 IS OBSOLETE
S/N 0102-LF-014-6601

SECURITY CLASSIFICATION OF THIS PAGE *(When Data Entered)*

403 617

the effects of finite chemical reaction rates. Two limiting cases corresponding to highly oblique confined flames and normal or unconfined oblique flames are treated. Of particular interest in the former case is the effect of the perturbations of the predicted orientation of the turbulent reaction zone. For the unconfined flames attention focuses on the effect of the perturbations on the turbulent flame speed and on the change in turbulent kinetic energy across the reaction zone. The characteristics of the related laminar flame are introduced so that the theory can conform to the practice of experimentalists in correlating their results for turbulent flame behavior in terms of such laminar flame characteristics. With respect to unconfined flames, for which considerable but often contradictory experimental data are available, the perturbation analysis appears to yield qualitative agreement with a recent correlation of experimental data showing the effect of turbulence Reynolds number. However, a comparison with results of individual experiments is inconclusive.